THE ROLE OF p120 RASGAP IN T CELLS AND LYMPHATICS

by

Philip E. Lapinski

A dissertation submitted in partial fulfillment
Of the requirements for the degree of
Doctor of Philosophy
(Immunology)
in The University of Michigan
2009

Doctoral Committee:

Associate Professor Philip D. King, Chair
Professor Benjamin L. Margolis
Professor Richard A. Miller
Associate Professor Kathleen L. Collins
Associate Professor Anne B. Vojtek

Acknowledgements

I would first like to thank my mentor, Phil King, for accepting me into his lab, and for all of his time and effort in training me to be a better scientist for the past six years. He is one of the smartest people I have ever met, is always available for discussions and questions, and his dedication to science is something to which I aspire. I also thank the current and former members of the King lab, especially Tim Bauler and Jen Oliver for their help, discussions, and friendships. They have made the King lab a place in which I thoroughly enjoy working.

There are many others who helped complete this work. I would like to thank Hanief Sofi from Cheong Hee Chang's lab for his generosity and advice. Grace Qiao, also from the Chang lab, performed the competitive bone marrow transfer experiments detailed in Chapter 3. Tom Glover, Matt Butler, and Susan Dagenais helped immensely by sharing the protocols and reagents for study of the lymphatic system of mice. Eva Sevick-Muraca and Sunkuk Kwon performed all of the near-infrared imaging described in Chapter 4. Thom Saunders and Elizabeth Hughes from the Transgenic Animal Model core performed the blastocyst injections and drug-selection of our embryonic stem cells during the generation of the RASA1 mouse. Eric Brown generously provided the Ub-Ert2-

Cre transgenic mice. I thank my thesis committee of Rich Miller, Ben Margolis, Anne Vojtek, and Kathy Collins.

Finally, I thank my wife Jackie for being so understanding of the demands of graduate school, being an outstanding mother, and for encouraging me to succeed. She has always supported me in my academic endeavors, and her work ethic has driven me to excel as a scientist.

Table of Contents

List of Figures

ABSTRACT

THE ROLE OF p120 RasGAP IN T CELLS AND LYMPHATICS

by

Philip E. Lapinski

Chair: Philip D. King

Ras is an intracellular signaling molecule that regulates many cellular processes in eukaryotic cells. Ras is activated by a class of proteins known as guanine nucleotide exchange factors (GEFs) and inactivated by GTPase-activating-proteins (GAPs). In T cells of the vertebrate immune system, the identity of the GEFs that activate Ras is known. In contrast, less is known about which GAPs inactivate Ras in this cell type. To learn more about the role of p120 RasGAP (RASA1) in the inactivation of Ras in T cells, we have generated a conditional RASA1-deficient mouse model. Using this model we have confirmed the role of RASA1 as a negative regulator of Ras in T cells. RASA1 controls not only activation of T cells in response to stimulation, but also helps to maintain their numbers in the peripheral immune system. The same mouse model has allowed us to establish that RASA1 is essential for the maintenance of lymphatic channels in mice which are necessary for T cell circulation through lymphoid organs and to sites of inflammation. In summary, we have established that RASA1 functions as an important physiological regulator of T cell function in vertebrates at multiple levels.

Chapter 1

Introduction

1.1 Ras family of G-proteins

Intracellular signal transduction induced by growth factors or a variety of other cell-activating ligands often involves activation of the proto-oncogene Ras, an evolutionarily-conserved, 21-kilodalton GTP-binding protein tethered to the inner leaflet of the cell membrane (1-4). The Ras-like superfamily of small G-proteins contains over 150 members in humans, including Ras, Rap1, Rap2, R-Ras, TC21, Ral, Rheb, and M-Ras. The Ras family of proteins is comprised of three functional members, including H-Ras, N-Ras, and K-Ras (5). Ras proteins act as GTP/GDP-controlled switches that are active when bound to GTP, and inactive when bound to GDP. Active Ras binds to multiple, distinct downstream effector molecules that mediate a number of signaling cascades which ultimately regulate cellular outcomes, such as survival, differentiation, and proliferation (2).

1.2 Ras signaling

In its active, GTP-bound state, Ras is recognized by effector molecules that include the serine kinase Raf-1, and the lipid/protein kinase

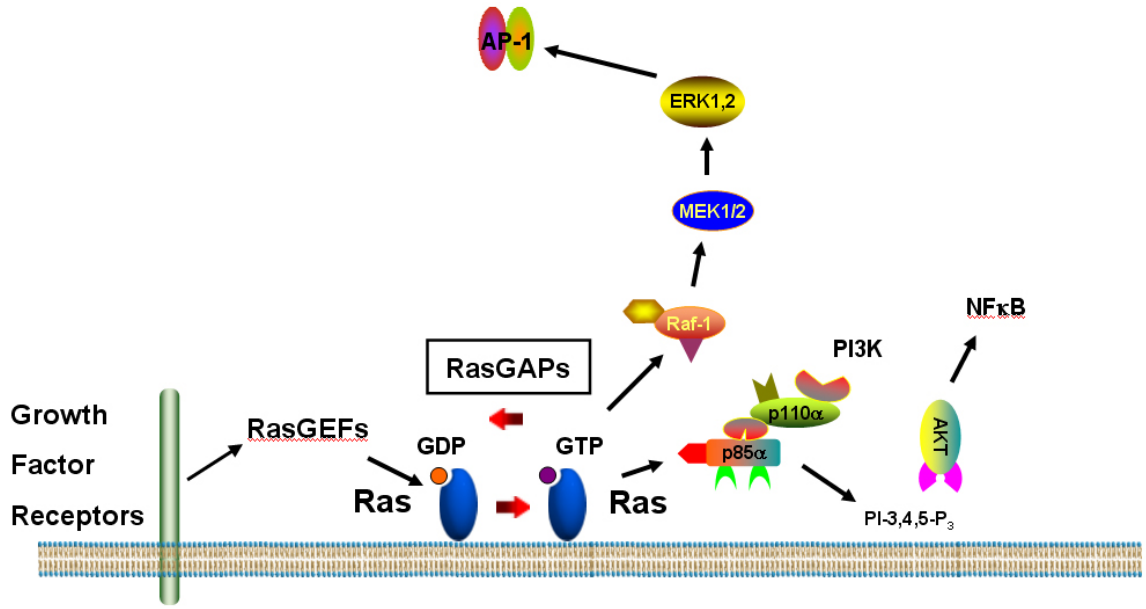

Figure 1: Function of RasGAPs in intracellular signal transduction. Following ligand interaction, growth factor receptors promote the recruitment to membranes of GEFs that switch Ras from an inactive GDP-bound to an active GTP bound state. Downstream effectors of Ras include Raf-1 and PI3K, which trigger activation of the MAPK signaling pathway and AKT, leading to nuclear mobilization of the AP-1 and NFκB transcription factors, respectively. RasGAPs perform the opposite function of GEFs and inactivate Ras. RasGAPs interact physically with Ras and increase its ability to hydrolyze GTP to GDP by several orders of magnitude.

phosphatidylinositol 3-kinase (PI3K) (6-8). Recognition of GTP-bound Ras by Raf-1 triggers the mitogen-activated protein kinase (MAPK) signaling cascade. This includes the phosphorylation of two MAPK kinases (MAP2Ks) called MEK1 and MEK2 by Raf-1. Once activated, MEK1 and MEK2 bind and phosphorylate the MAPKs, extracellular signal regulated kinase 1 and 2 (ERK1 and ERK2), which then translocate to the nucleus. ERK1 and 2 subsequently phosphorylate components of the AP-1 transcription factor, leading to their assembly and activation (9) (Figure 1). PI3K recognition of GTP-bound Ras results in the generation of PI-3,4,5-P_3 in membranes, resulting in the membrane recruitment

and activation of the serine kinase AKT (10). AKT triggers activation of the transcription factor NFκB, thus regulating signaling pathways related to cell survival. Through regulation of these different pathways, Ras plays an important role as a mediator of cell growth, proliferation, and differentiation.

1.3 Regulation of Ras activity

As Ras plays an integral role in a multitude of cellular processes, its activity must be tightly regulated. Ras has an extremely slow endogenous rate of GTP hydrolysis and GDP exchange, which is too slow for Ras to effectively be activated or downregulated after stimulation without the help of other regulators. Therefore, Ras is controlled by two different types of regulatory proteins (11). Guanine nucleotide exchange factors (GEFs) function to eject GDP from the nucleotide-binding site of Ras, which allows GTP to bind, because GTP is present at higher intracellular concentrations than GDP (1, 2, 11). Well-characterized examples of GEFs include son of sevenless (SOS) and Ras guanyl nucleotide-releasing protein 1 (RasGRP1) (11). To control the inactivation of Ras, a class of proteins known as GTPase-activating proteins (GAPs) physically associates with Ras-GTP and enhances the endogenous GTPase activity of Ras by several orders of magnitude (12-15). At least ten different GAPs have been discovered in mammals, including the prototypical RasGAPs neurofibromin 1 (NF1) and p120 RasGAP (RASA1) (5, 12, 13). Ras is known to be an oncogene, with approximately 25% of all human tumors harboring a mutated form of Ras,

Figure 2: Domain organization of RASA1. Relative positions of the SH2, SH3, PH, C2, and GAP domains are indicated.

with some forms of tumor having a Ras mutation in as many as 90% of cases (14,16). The mutation usually renders the protein refractory to GAP activity, leaving Ras trapped in an activated state. These percentages are likely to be an underestimation of the importance of Ras signaling in tumors, however, as aberrant Ras signaling can occur without mutations of Ras itself (17).

1.4 RASA1 structure

RASA1 was the first RasGAP to be characterized at the molecular level (18). The RASA1 molecule is composed of six modular domains (Figure 2). These include two Src-homology-2 (SH2) domains and a Src-homology-3 (SH3) domain (which recognize phospho-tyrosine residues and proline-rich sequences, respectively), a pleckstrin homology (PH) and PKC2 homology (C2) domain (both implicated in membrane phospholipid binding, the latter in a calcium-dependent manner), and a GAP domain, which confers GTPase-enhancing activity. One or more of these domains are predicted to mediate recruitment of RASA1 to membranes, this serves to locate the GAP domain in the vicinity of Ras-GTP. For example, the SH2 domains of RASA1 are implicated in membrane targeting of RASA1 during platelet-derived growth factor (PDGF) and epidermal growth factor (EGF) signaling in fibroblasts, through recognition of phosphorylated tyrosine residues in the respective receptors (19-22). RASA1 itself has been

shown to be tyrosine phosphorylated by several different protein tyrosine kinases in a number of cell types. However, the stoichiometry of phosphorylation is generally low, and no change in subcellular localization or activity of RASA1 upon tyrosine phosphorylation has been observed (18).

1.5 Control of Ras by RASA1

Since the association of RASA1 with growth factor receptors is inducible, RASA1 is likely a negative-feedback regulator of Ras, rather than a constitutive negative-regulator. Chemical reaction constants for the interaction of the RASA1 GAP domain and Ras-GTP show an optimal GAP activity at high Ras-GTP concentrations, further suggesting a negative-feedback role for RASA1 (23). In RASA1-deficient mice, this hypothesis has been confirmed, at least for PDGF-signaling in fibroblasts. Fibroblasts have been isolated from RASA1-deficient embryos (see below), and Ras activation in response to PDGF has been examined *in vitro* (24). When stimulated by PDGF, Ras-GTP levels are elevated two-fold in RASA1-deficient fibroblasts compared to wild type. However, in the resting state, Ras-GTP levels are equivalent in RASA1-deficient and wild type cells, suggesting that RASA1 controls the level of Ras-GTP only upon stimulation.

1.6 Ras-independent functions of RASA1

In addition to controlling Ras activation, RASA1 also controls certain cellular functions in a GAP domain-independent and a Ras-independent manner.

For example, RASA1 has been implicated in the control of cell motility. Directed cell movement in RASA1-deficient embryonic fibroblasts (see below) is impaired, and appears to require an interaction of RASA1 with the p190 RhoGAP protein. This interaction is mediated by the SH2 domains of RASA1 (24-26). p190 RhoGAP acts as a GAP for the Rho family of small G-proteins, which are known to regulate the formation of focal adhesions and actin fibers necessary for directed cell movement (27).

Another GAP-domain independent function of RASA1 is the regulation of apoptotic cell death. In fibroblasts subjected to mild apoptotic stress, RASA1 is cleaved by activated Caspase 3, and the free N-terminal fragment is able to directly activate AKT via its SH2 and SH3 domains (28-31). Under these conditions, RASA1 is thought to provide anti-apoptotic signals that permit survival of the stressed cell. However, under more severe apoptotic stress, the N-terminal fragment of RASA1 is further cleaved by Caspase 3, resulting in two shorter N-terminal fragments. The result of this cleavage is a reduction in AKT activity, which leads to efficient apoptotic death of the cell. Therefore, the second cleavage event of RASA1 functions to abrogate the anti-apoptotic function of the longer N-terminal fragment.

1.7 RASA1-deficient mice

A null allele of mouse *rasa1* has been generated, but mice homozygous for the null allele die at embryonic day 10.5 (E10.5) (32). These mice develop normally until E9.25, when they display a defect in posterior elongation, and by

E9.5 are significantly smaller than littermate controls. This is most likely due to a severe vascular developmental defect, in which blood vessel endothelial cells fail to organize into a vascular network in the yolk sac. The blood vasculature in the embryo proper is also affected, and ultimately develops local ruptures leading to leakage of blood into the body cavity. Eventually the pericardial sac becomes distended, leading to a labored heartbeat and reduced blood flow. RASA1-deficient embryos also display extensive apoptotic cell death in the brain, with large numbers of dead and dying cells as early as E9.0 in the hindbrain, optic stalk, and telencephalon.

1.8 RASA1 mutations in humans

A recently described human clinical disorder known as capillary malformation-arteriovenous malformation (CM-AVM) has been shown to be caused by mutations of the *RASA1* gene (33-36). This condition is characterized by multiple randomly distributed pink lesions that result from the malformation of skin capillaries. Approximately one third of patients develop fast-flow vascular lesions, including Parkes-Weber Syndrome, arteriovenous fistulas, and intracranial arteriovenous malformations. Arteriovenous fistulas are abnormal connections between arteries and veins, where the two are directly connected without branching into capillaries, and Parkes-Weber Syndrome is characterized by cutaneous flush, and multiple underlying arteriovenous fistulas. It is also associated with soft tissue and skeletal hypertrophy, usually of an affected limb. Thus far, one hundred forty individuals with RASA1 mutations have been

identified, and all but six of these have CM-AVM. Forty-two different mutations in the RASA1 gene have been described, including insertions and deletions resulting in frame-shifts, disruption of splice sites, and nonsense, missense, or splice-site substitutions. The mutations are randomly distributed throughout the RASA1 gene, and only one germline RASA1 gene is affected in CM-AVM patients (mutation of both alleles of RASA1 would presumably result in embryonic lethality). CM-AVM is hypothesized to arise from loss of function of the intact RASA1 allele by somatic mutation, which is consistent with the focal nature of the lesions. At least two CM-AVM patients have developed chylothorax or chylous ascites, rare conditions in which lipid-laden lymph fluid, or chyle, leaks from lymphatic vessels into the thoracic or abdominal cavities, respectively (36). Thus, RASA1 has been found to play a role in the formation and maintenance of the blood and/or lymph vasculature in both mice and humans.

1.9 TCR signaling

T cells comprise one arm of the vertebrate adaptive immune system. These cells act by recognizing antigenic peptides in the context of a Major Histocompatibility Complex (MHC) molecule expressed on the surface of an antigen-presenting cell. MHC molecules are divided into two classes, MHC Class I and MHC Class II. MHC Class I molecules are expressed on virtually all nucleated cell types, and typically present antigens derived from proteins produced in the cytoplasm of the presenting cell, and are recognized by CD8+ T cells (37). MHC Class II molecules are primarily expressed by professional

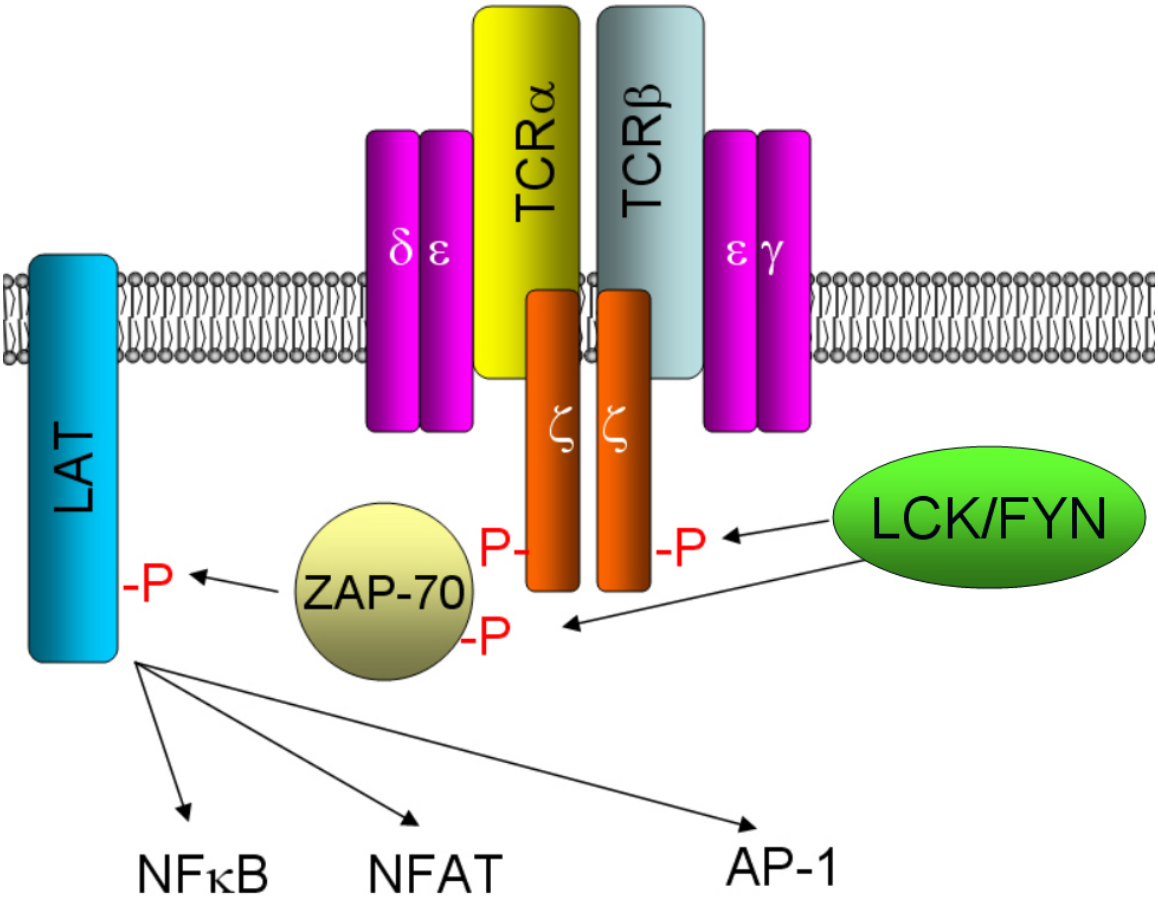

Figure 3: Proximal events in TCR signaling. Upon TCR ligation with cognate MHC/peptide complex, the TCRζ chains are phosphorylated on their ITAM motifs by the tyrosine kinases LCK and FYN. ZAP-70 is then recruited to the phosphorylated ITAMs, where it is itself phosphorylated by LCK. The activated ZAP-70, which itself is a tyrosine kinase, phosphorylates LAT which serves to transduce signals which culminate in the activation of the NFκB, NFAT, and AP-1 transcription factors.

antigen-presenting cells, such as dendritic cells or B cells, and usually present antigens from outside of the presenting cell that have been phagocytosed by the antigen-presenting cell. MHC Class II molecules are recognized by CD4+ T cells. Recognition of the peptide/MHC is the role of the T Cell Receptor (TCR). The TCR is composed of an α and β chain, which each contain a constant and a variable region and are generated through random re-arrangements of gene

segments (38). The TCR ζ chains, as well as CD3 δ and ε chains associate with the TCR α and β chains, and contain immunoreceptor tyrosine-based activation motifs (ITAMs), which are phosphorylated upon T Cell Receptor (TCR) engagement (Figure 3). When the TCR is engaged, the SRC-family kinases LCK and FYN are rapidly activated and phosphorylate ITAMs on the CD3 and TCRζ chains of the TCR complex. The phosphorylated ITAMs are recognized by the protein tyrosine kinase ZAP-70. Upon ZAP-70 recruitment to phosphorylated ITAMs, ZAP-70 itself is phosphorylated and activated by LCK. Activated ZAP-70 phosphorylates a restricted set of substrates, including the adapter proteins LAT and SLP-76 (8, 39). These adapter proteins act in concert to activate PLCγ1, which catalyzes the hydrolysis of Phosphatidylinositol (PI)-4,5-P_2 to generate diacylglycerol (DAG) and inositol-1,4,5-P_3 (IP_3). The presence of IP_3 leads to calcium mobilization and subsequent activation of the transcription factor NFAT by Calcineurin. The RasGEF RasGRP1 is recruited to the inner leaflet of the membrane by the presence of DAG, where it can catalyze the activation of Ras. This leads to the activation of the MAPK pathway, and ultimately the activation of c-Fos (40-42). SOS is another RasGEF that is known to activate Ras in T cells, and it is localized to activated LAT by its association with the adapter protein Grb2. LAT also associates with PI3K, which phosphorylates PI-4,5-P_2 (PIP_2) to generate PI-3,4,5-P_3 (PIP_3). The serine/threonine kinase AKT is activated by PIP_3, and through its interaction with the DAG-responsive serine/threonine kinase PKCθ activates the transcription factors NFκB and c-Jun. The transcription factor AP-1 is composed of a heterodimer of c-Fos and c-Jun family

proteins. Ultimately, the transcription factors AP-1, NFκB, and NFAT are the major factors that are activated by T cell signaling, and these factors act cooperatively to induce transcription of genes involved in cell proliferation, differentiation, and cytokine secretion.

1.10 T cell development

T cell precursors develop in the bone marrow from hematopoietic stem cells, and migrate to the thymus to mature (43). T cells undergo three distinct selection events during maturation. The first event is when T cell precursors, expressing neither the CD4 nor CD8 co-receptors (Double-Negative, DN) rearrange their TCR β chain, which is expressed on the cell surface with a surrogate pre-α chain (44). The DN stage of development can be separated into four distinct stages, DN1 through DN4, which are defined by the alternate expression of the CD44 and CD25 markers (DN1 = CD44-hi, CD25-lo, DN2 = CD44-hi, CD25-hi, DN3 = CD44-lo, CD25-hi, DN4 = CD44-lo, CD25-lo) (45). It is at the DN3-DN4 transition that the T cell precursor expresses the pre-TCR. The successful expression of the pre-TCR signals the cell to begin expressing the CD4 and CD8 co-receptors (Double Positive, DP), at which point the cells begin to proliferate. The large majority of cells in the thymus are in the DP stage of development (46). When proliferation ceases, the DP cells rearrange the TCRα chain, which is expressed on the cell surface in a complex with the TCRβ chain. At this point in development, the ability of the TCR to recognize self-MHC molecules conjugated to self-peptides is tested in a process known as positive

selection. Cells expressing a TCR that cannot recognize self-MHC/peptide die by neglect, while cells that do recognize self-MHC/peptide survive (47). If the TCRs of the DP thymocytes recognize MHC Class I, the cells stop expressing CD4 and mature into CD8+ cells. Conversely, if MHC Class II is recognized by the TCR, the cells cease expression of CD8 and become CD4+ cells (48). At the same time, the cells undergo the process of negative selection, where cells that express a TCR that binds too strongly to self-MHC/peptide complexes are deleted from the repertoire in order to prevent autoimmunity (49). The selection regimen in the thymus generates a repertoire of T cells capable of responding to a multitude of antigenic peptides in the periphery, and that do not react to self-antigens. When mature T cells leave the thymus, they are known as naïve, becuase they have not yet encountered their cognate antigen.

1.11 Mature T cell function

Approximately 1 % of DN thymocytes in the thymus survive the selection process and mature into T cells (50). Mature T cells migrate from the thymus into the peripheral lymphoid organs, such as the lymph nodes and spleen. CD8+ T cells, known as cytotoxic T (T_C) cells, function to recognize and kill tumor cells or virus-infected cells by inducing cell death by apoptosis (51). CD4+ cells are broadly known as T Helper (T_H) cells and primarily function to secrete cytokines which activate other immune cell types. What type of immune response is stimulated depends on the subtype of T_H cell that the naïve CD4+ cell differentiates into when activated. T_H1 cells produce the cytokines IFNγ, TNFα,

and TNFβ, and activate cell-mediated immunity by activating macrophages and stimulating B cells to produce opsonizing antibodies, predominantly the IgG class (52). T_H2 cells secrete the cytokines IL-4, IL-5, IL-6, and IL-13, and stimulate humoral responses by activating B cells to produce IgM, IgA, and IgE classes of antibody (52). T_H1 responses are primarily raised against intracellular pathogens, including viruses or intracellular parasites such as *Leishmania* and *Toxoplasma gondii*, while T_H2 responses provide protection against extracellular pathogens, including intestinal helminths (53). Other subclasses of CD4+ cells include the CD4+ CD25+ T regulatory cells (T_{reg}) and the recently discovered T_H17 cells. Instead of stimulating an immune response, T_{reg} cells suppress inflammation and autoimmunity by secreting TGFβ and IL-10 when stimulated. Depletion of the Treg population in mice results in multi-organ specific autoimmunity, and also increases immunity to tumors, grafts, allergens and pathogens (54). T_H17 cells have been found to be important in autoimmunity and tissue inflammation due to their secretion of the cytokines IL-17, IL-17F, and IL-22. In addition, they have been suggested to play a role in the clearance of a number of pathogens, including *Mycobacteria* and *Pneumocystis carinii* (55).

In order for a T cell to be activated through its TCR, the cell must also receive a second signal from the same antigen presenting cell that expressed the stimulatory MHC/peptide complex. This co-stimulatory signal is transduced through the interaction of CD28 on the T cell and a B7 molecule on the antigen presenting cell (46). Antigen presenting cells are induced to produce B7 molecules by detecting the presence of infection through receptors of the innate

immune system, including Toll-like receptors. The requirement for a second signal to activate the T cell ensures that only T cells that are specific for an antigenic peptide presented by an antigen presenting cell during an infection are activated, and not T cells that recognize self antigens on non-infected cells.

When a naïve T cell is activated by an antigen-presenting cell by engagement of the TCR with MHC/peptide complex, and by co-stimulation of the CD28 receptor, the cell begins to divide rapidly. This proliferation serves to vastly increase the numbers of T cells that are capable of responding to that particular antigen. After the activated T cells have proliferated, they mature into effector T cells, and carry out their respective immune functions by secreting cytokines and killing infected cells. Once the antigen has been cleared, the majority of the short lived antigen-specific effector T cells die by apoptosis. However, a significant number of antigen-specific T cells persist in secondary lymphoid organs as long-lived memory T cells, which are the basis of immunological memory. These cells ensure that if the antigen is encountered again, the T cell response will be faster and more vigorous than the initial response, and provide lasting protective immunity (46).

1.12 Ras signaling in T cell development

The importance of Ras/MAPK signaling in T cell development in the thymus is well documented. Retrovirus infection of fetal thymic organ cultures with viruses driving expression of constitutively-active or dominant-negative MEK1 have shown that the ERK pathway is critical to the differentiation of DN3

thymocytes (56). The critical role of ERK1/2 in thymocyte development has been further illustrated by the use of ERK1 and ERK2-deficient mice (57, 58). ERK1-deficient mice display a partial arrest in T cell development at the DP stage, and mice in which ERK2 is specifically deleted early in thymocyte development show a partial block in development from the DN3 to DN4 stage. Thymocytes which are deficient in both ERK1 and ERK2 are nearly completely blocked at the positive selection stage of development.

1.13 Ras signaling in mature T cells

Ras/MAPK signaling is known to be important to many aspects of mature T cell function (59, 60). Mature T cells deficient in ERK2 proliferate markedly less vigorously than wild type cells when stimulated with αCD3 antibodies, and show decreased survival after stimulation (61). Ras signaling has also been shown to be a critical component in the secretion of the T cell growth factor IL-2 upon T cell activation. By transfecting either a constitutively-active or dominant-negative form of Ras into a T cell line, the secretion of IL-2 upon cell stimulation was enhanced or inhibited, respectively (62, 63).

Anergy is a persistent, unresponsive state of T cells that is a result of TCR signaling without the CD28 co-stimulatory signal. This process is thought to mediate self-tolerance by inactivating self-reactive T cells. Anergy is characterized by the inability of T cells to secrete IL-2 upon stimulation, and defective AP-1 transactivation. Ras/MAPK activation was found to be inhibited upon TCR stimulation of anergic T cells (64, 65). This is suggested to be due to

an inability of RasGRP1 to be recruited to the inner leaflet of the membrane of anergic cells, and a subsequent inability to activate Ras (66).

1.14 RASA1 function in T cells

The role of RASA1 in T cells has never been directly demonstrated, at least partially due to the fact that RASA1-deficient mice succumb *in utero*. The ablation of the related RasGAP NF1 in mice also causes embryonic lethality, NF1-deficient mice die at embryonic day 14.5 (67). However, the effect of NF1-deficiency on T cells was studied by adoptive transfer of NF1-deficient fetal liver cells into irradiated recipient mice. Introduction of these NF1-deficient hematopoietic stem cells was associated with thymic and splenic hyperplasia and increased constitutive Ras-GTP levels (68). However, Ras-GTP levels were not found to be increased in NF1-deficient T cells upon TCR signaling, indicating that NF1 is a constitutive negative-regulator of Ras in these cells. Unfortunately, RASA1-deficient T cells cannot be studied in this way, because of the earlier embryonic death of RASA1-deficient embryos. To circumvent this problem, we have generated a conditional RASA1-deficient mouse model.

1.15 Generation of conditional alleles

Non-conditional gene-targeting technology is an extremely powerful tool for the elucidation of the functions of genes. In this method, the gene of interest is inactivated in all tissues by disrupting an exon predicted to be critical to gene function. Typically, this is performed by inserting a Neomycin-resistance gene

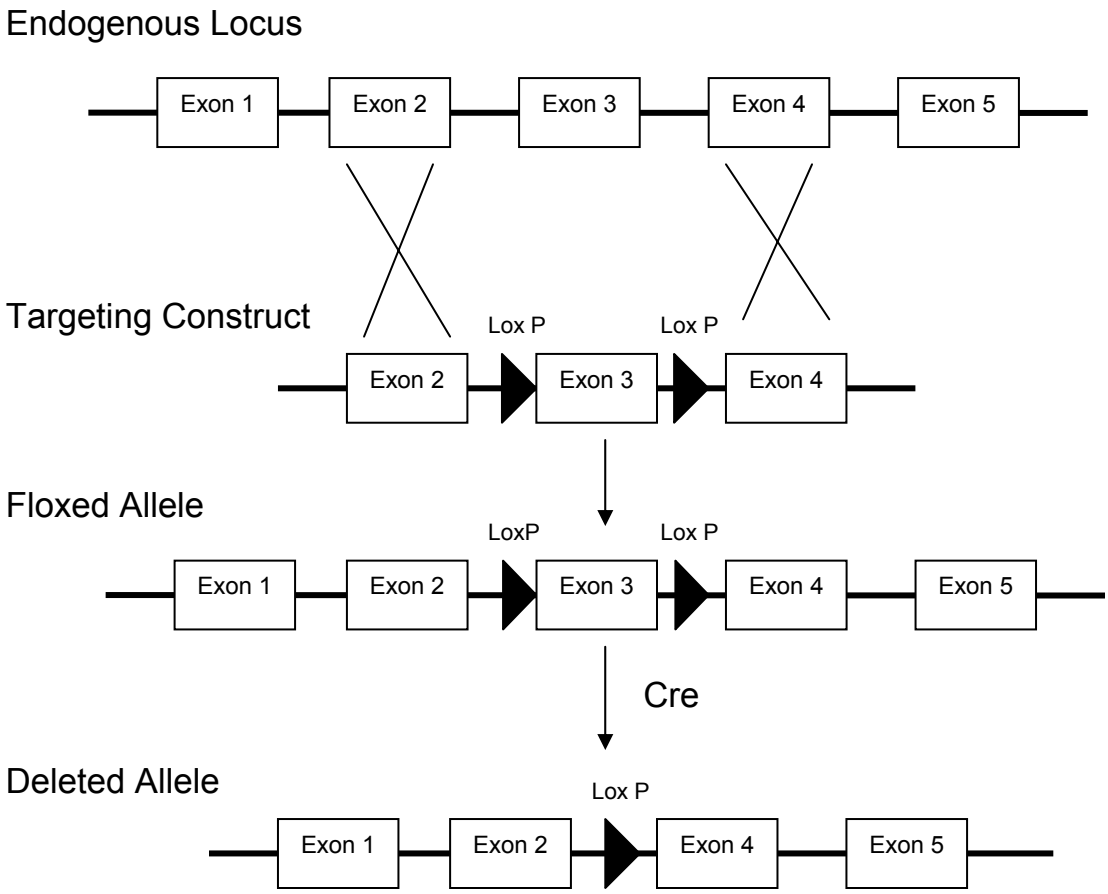

Figure 4: Conditional gene targeting. A targeting construct in which the exon to be deleted (exon 3 in this case) is flanked by loxP sites (floxed). The targeting construct is electroporated into ES cells, and can recombine with the endogenous locus by homologous recombination. Mice bearing the floxed allele are then crossed to mice expressing the Cre recombinase under control of a tissue-specific or drug inducible promoter. The recombinase recognizes the loxP sites and splices out the floxed exon, disrupting gene expression.

into a critical exon. Alternatively, the critical exon can simply be replaced by a Neomycin-resistance gene. The targeted disruption is achieved by generation of a DNA targeting construct in which a Neomycin-resistance gene is inserted into the target DNA sequence, and is flanked by regions homologous to the target sequence. This construct is then transfected into embryonic stem (ES) cells, where it can integrate into the genome by homologous recombination. The ES

cells containing the targeted allele are selected by culture in Neomycin, and are subsequently injected into blastocysts (32 cell stage embryos), where they can contribute to the development of tissues, including the germ cells. By crossing these chimeric animals, mice which are homozygous for the null allele, and therefore do not express the targeted protein, can be produced (69). This system, while powerful, has potential drawbacks. The deletion of one or both copies of genes important to embryonic development can cause embryonic lethality, making study of the protein of interest in adult animals more difficult. In addition, since the protein of interest is deleted in all tissues, questions can be raised about the origin of observed phenotypes. For example, if T cells are found to be affected in a gene-targeted mouse, it can be difficult to determine if the defect is intrinsic to T cells, or if it is secondary to a developmental defect in T cells caused by a defect in thymic epithelial cells.

In order to circumvent this problem, a method to delete a gene of interest in specific tissues, or in an inducible manner, was developed. This method utilizes the Cre-loxP system from bacteriophage P1 (70, 71) (Figure 4). In this system, an exon of the gene of interest is targeted with a DNA targeting construct, but instead of inserting a NeoR cassette, the exon of interest is flanked by loxP sites (floxed), which are 34bp recognition sites that can be recognized by the Cre recombinase. When Cre recombinase recognizes the two loxP sites, they are spliced together, deleting the exon between them. The loxP sites are small enough not to interfere with normal exon splicing during mRNA processing, so gene expression of the floxed, non-deleted allele is typically unaffected. The

conditional targeting construct is then transfected into ES cells, and the screening, blastocyst injection, and breeding process is similar to that of complete knockout animals. By crossing mice that are homozygous for the floxed allele with transgenic (Tg) mice expressing Cre recombinase under the control of a tissue-specific or inducible promoter, a mouse model in which the gene of interest can be specifically deleted in certain tissues or at certain times during development can be achieved. This system permits circumvention of the problem of potential embryonic lethality, as expression of the protein of interest can be disrupted only in tissues not critical to embryonic development. In addition, the deletion of the protein of interest in specific cell types allows any observed phenotypes to be directly attributed to that cell type, since all other tissues express the targeted protein normally.

1.16 Scope of the Thesis

The above background provides a framework for understanding the central questions of this thesis. Using a conditional RASA1-deficient mouse model, we examine the effect of RASA1-deficiency on the development and function of T cells, as well as in other immune and non-immune tissues. In Chapter 2, the construction of the conditional RASA1 allele and initial analysis of the conditional RASA1-deficient mouse model is detailed. In Chapter 3, we analyze RASA1-deficient T cells by crossing conditional RASA1-deficient mice with mice expressing a T cell-specific Cre recombinase. By using *in vivo* and *in vitro* techniques, we describe the importance of RASA1 in the normal function of

T cells. In Chapter 4, a drug-inducible form of Cre that is expressed in all tissues is utilized to examine the effect of complete RASA1-deficiency induced in adult animals. Biochemical techniques as well as fluorescence microscopy and imaging are used to characterize a defect in the lymphatic system of these mice. This model has revealed that, in adult animals, RASA1 is required for the normal functioning of T cells and of lymphatic vessels that allow the circulation of immune cells between tissues, lymphoid organs, and blood.

Chapter 2

Generation of mice with a conditional allele of *rasa1*

2.1 Abstract

p120 Ras GTPase-activating protein (RasGAP or RASA1) encoded by the *rasa1* gene in mice is a prototypical member of the RasGAP family of proteins involved in negative-regulation of the p21 Ras proto-oncogene. RASA1 has been implicated in signal transduction through a number of cell surface receptors. In humans, inactivating mutations in the coding region of the RASA1 gene cause capillary malformation arteriovenous malformation. In mice, generalized disruption of the *rasa1* gene results in early embryonic lethality associated with defective vasculogenesis and increased apoptosis of neuronal cells. The early lethality in this mouse model precludes its use to further study the importance of RASA1 as a regulator of cell function. Therefore, to circumvent this problem, we have generated a conditional *rasa1* knockout mouse. In this mouse, an exon that encodes a part of the RASA1 protein essential for catalytic activity has been flanked by loxP recognition sites. With the use of different constitutive and inducible Cre Tg mouse lines, we show that deletion of this exon from the *rasa1* locus results in effective loss of expression of

catalytically-active RASA1 from a variety of adult tissues. The conditional *rasa1* mouse will be useful for the analysis of the role of RASA1 in mature cell types.

2.2 Introduction

Ras is a small inner membrane-localized GTP-binding protein that controls numerous cell processes including growth, death, differentiation, migration and polarity (3, 4). Activating mutations of Ras are observed commonly in human cancer (14). Ras is active in its GTP-bound state and inactive in its GDP bound state that results from Ras hydrolysis of GTP. In its GTP-bound form, Ras triggers the activation of Ras effector molecules such as Raf-1 and phosphatidylinositol 3-kinase (6, 7). The intrinsic GTPase activity of Ras is low and is considered constant. Instead, other proteins are thought to control the ratio of Ras-GTP to Ras-GDP during cellular signal transduction. One such class of Ras-regulating proteins are GEFs (11). Upon juxtaposition to Ras, GEFs eject GDP from the Ras guanine nucleotide-binding pocket. Since the concentration of GTP is higher than that of GDP in the cytosol, the evacuated Ras preferentially binds GTP, resulting in Ras activation. Another class of Ras-regulating proteins are the RasGAPs (11, 13). RasGAPs increase the ability of Ras to hydrolyze bound GTP by several orders of magnitude, resulting in Ras inactivation.

A number of RasGAPs have now been described including neurofibromin, RASA1-4, RASAL1 and L2, and SynGAP (11, 12). Amongst these, neurofibromin and RASA1 are the prototypical members. Like other RasGAPs, RASA1 contains several modular binding domains in addition to its GAP domain.

These include two Src homology-2 (SH2) domains, an SH3 domain, and pleckstrin homology (PH) and protein kinase C2 homology domains (Figure 5). These domains are thought to mediate recruitment of RASA1 to receptors and membranes whereupon it becomes localized to Ras. As a negative-regulator of Ras, RASA1 has been implicated in signal transduction though numerous receptors, e.g. PDGF, epidermal growth factor, ephrin, insulin, colony stimulating factor-1 and T cell antigen receptors (19, 72-76). In addition, RASA1 has been shown to regulate cell death in response to mild genotoxic stress through Ras-independent mechanisms (28, 30).

Recently, inactivating mutations of the human RASA1 gene have been shown to cause a novel clinical disorder named CM-AVM (33, 34). Furthermore, a targeted null mutation of *rasa1* in mice causes early embryonic lethality (E10.5) associated with vascular defects and increased apoptotic cell death in developing brain (32). These findings suggest an important physiological function for RASA1 at least in endothelial cells and neuronal cells.

Studies of fibroblasts derived from *rasa1* mutant embryos have additionally revealed a role for RASA1 in directed movement and in PDGF receptor signal transduction in this cell type (24, 25). However, because of early embryonic lethality of the *rasa1* mutant mice, it has not been possible to use these mice as a model with which to further study the influence of inactivation of RASA1 expression in adult tissues. To this end, we generated a conditional allele of *rasa1* in mice.

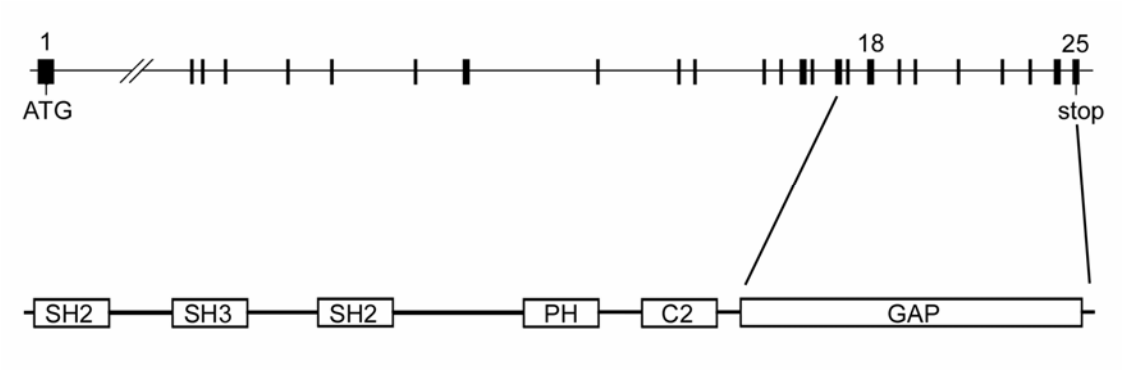

Figure 5: Genomic organization of *rasa1* and domain structure of RASA1. At top is depicted the intron/exon organization of *rasa1* spanning 74 kbp on chromosome 13. The 25 exons are shown as vertical bars. Below is a representation of the RASA1 protein showing modular binding domains and the GAP domain. The GAP domain is encoded by exons 16-25 of the RASA1 gene. Exon 18 of *rasa1* encodes the Arginine finger loop region of the GAP domain essential for catalytic activity.

2.3 Targeting strategy

The *rasa1* gene contains 25 exons, of which exon 18 encodes the entire arginine finger loop region of the GAP domain essential for accelerated Ras hydrolysis of GTP (Figure 5). Therefore, as a targeting strategy, we attempted to flank exon 18 with loxP sites (Figure 6). Following excision of exon 18 by Cre-mediated recombination, mutant *rasa1* transcripts would, at the most, be expected to direct the expression of catalytically-inactive RASA1 molecules that lack a functional GAP domain. Furthermore, nonsense sequences would be contained in transcripts from this allele as exon 17 would remain unspliced or spliced to downstream exons, all of which are out of frame with exon 17. Theoretically, therefore, transcripts could be rapidly degraded by nonsense-mediated RNA decay, resulting in complete loss of RASA1 expression (76).

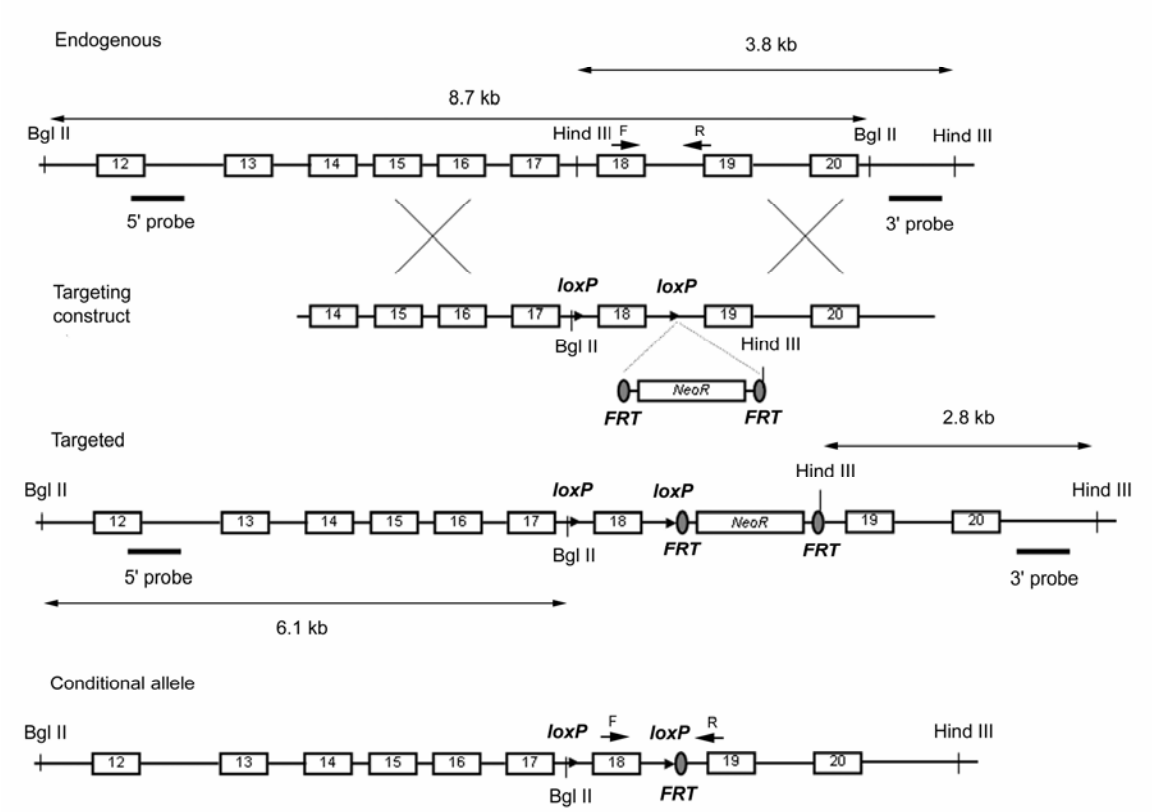

Figure 6: Generation of a conditional *rasa1* allele. At top is shown the organization of part of the endogenous *rasa1* gene and targeting construct used to generate a targeted *rasa1* allele in ES cells. The structure of the targeted allele and a conditional *rasa1* allele that results from Flp-mediated excision of the *NeoR* cassette is shown below. Locations of restriction sites, 5' and 3' DNA probes and PCR primers used for Southern blotting and genotyping are indicated.

2.4 Construction of the conditional allele

A *rasa1* targeting construct in which loxP sites were inserted on either side of exon 18 and a neomycin resistance gene cassette (NeoR) flanked by FRT sites was inserted downstream of the 3' loxP site in intron 18 was electroporated into W4 embryonic stem (ES) cells (Figure 6). Following neomycin selection, correctly-targeted clones were identified by Southern blotting (Figure 7). Two such euploid clones were used to generate chimeric mice, which were bred with C57BL6/J mice to achieve germline transmission of the targeted allele. Deletion

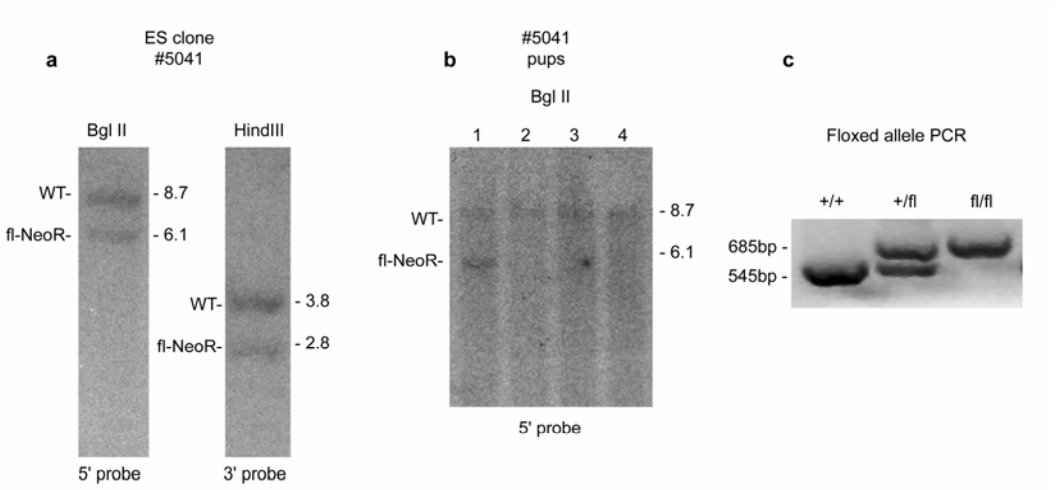

Figure 7: Southern blotting and PCR genotyping of targeted and conditional *rasa1* alleles. (A) Neomycin-resistant ES cell clones were screened for correct targeting of *rasa1* by Southern blotting of genomic DNA. Shown are Southern blots of one of several correctly-targeted clones using the indicated restriction enzymes and probes (see Figure 6). **(B)** The ES clone shown in (a) was used to generate chimeric mice, which were bred with wild type C57BL/6 mice to achieve germline transmission of the targeted allele. Shown is a Southern blot of tail DNA from four littermate pups from this cross. Pup 1 has inherited the targeted allele. **(C)** Mice with a targeted *rasa1* allele were crossed with *actin-FLP* Tg mice to delete the *NeoR* cassette. Resulting heterozygote *rasa1* floxed mice were intercrossed to generate wild type, heterozygote and homozygote *rasa1* floxed progeny. Genotype was determined by PCR of tail DNA using forward and reverse primers shown in Figure 6. PCR products of 685 and 545 bp are generated from *rasa1* floxed and wild type alleles, respectively.

of the NeoR cassette from the targeted allele was then achieved by breeding of heterozygote targeted mice with C57BL6/J mice carrying a Flp transgene under control of an actin promoter (77). This allowed the generation of mice with conditional *rasa1* floxed (fl) alleles (Figure 7).

2.5 Disruption of RASA1 expression by pLCK-Cre

To demonstrate disruption of RASA1 expression, *rasa1*$^{fl/fl}$ mice were crossed with Tg mice that express Cre in different immune cell lineages. Cre Tg lines examined included pLCK-Cre (T cell lineage), CD19-Cre (B cell lineage) and LysM-Cre (myeloid lineage) (78-80). Shown are the results of anti-RASA1 Western blots of whole thymus and spleen cell suspensions from pLCK-Cre Tg mice homozygous for wild type or floxed *rasa1* alleles (Figure 8). In thymi of *rasa1*$^{fl/fl}$ *pLCK-Cre* mice, expression of full-length RASA1 was almost extinguished. Of the trace amounts of protein that remained, this could be accounted for by the presence in thymus of non-T lineage cells such as macrophages, dendritic cells and epithelial cells that would not be expected to express Cre (~2–5% of total thymic cells). Less RASA1 deletion was noted in whole spleen (Figure 8). However, this is consistent with the fact that T cells comprise only 20–30% of total splenocytes. In lymph node (LN), for example, where T cells comprise 60–70% of total cells, levels of RASA1 expression are reduced correspondingly, consistent with almost complete loss of RASA1 expression in the T cell lineage (not shown). Similar to results obtained with pLCK-Cre, homozygous *rasa1*$^{fl/fl}$ mice with CD19-Cre or LysM-Cre transgenes express much reduced levels of full-length RASA1 protein in splenic B cells and in bone-derived macrophages, respectively (not shown). Experiments aimed at understanding the consequences of RASA1 loss in different immune cell lineages are discussed in Chapter 3. We show that while RASA1 appears to be dispensable for function of macrophages and B cells, it performs a critical role in the development and function in T cells.

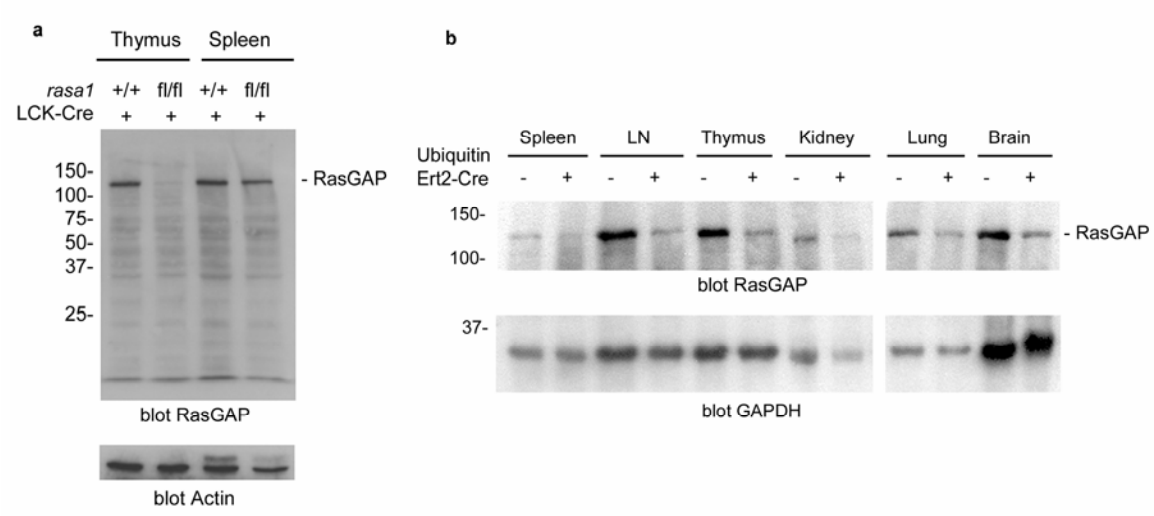

Figure 8: RASA1 protein expression in *rasa1*$^{fl/fl}$ Cre-transgenic mice. (A) RasGAP protein expression in thymus and spleen of *pLCK-Cre* Tg wild type and homozygote *rasa1*$^{fl/fl}$ mice was determined by Western blotting using a RASA1 antibody that reacts with the NH_2-terminal SH2 and SH3 domains of RASA1. Blots were reprobed with an actin antibody to verify equal protein loading. Note the almost complete loss of expression of RasGAP in thymus of the *rasa1*$^{fl/fl}$ mice. Note also that no unique lower molecular mass RASA1 antibody-reactive bands are present in *rasa1*$^{fl/fl}$ lanes. Identical results were obtained with an antibody that is specific for the RasGAP SH3 domain (not shown). **(B)** Homozygote *rasa1*$^{fl/fl}$ mice with or without an inducible *Ub-Ert2-Cre* transgene were injected with tamoxifen intraperitoneally on two consecutive days. Seven days later mice were sacrificed and expression of RASA1 in different tissues was determined by Western blotting as in **(A)**. Equivalent protein loading was demonstrated by reprobing of blots with a GAPDH antibody.

2.6 Disruption of RASA1 expression by Ub-Ert2-Cre

Mice with a *rasa1*$^{fl/fl}$ allele were also crossed with mice that carry an inducible *Ert2-Cre* transgene under the control of a ubiquitin (Ub) promoter (81). In this model, the Cre recombinase is expressed in all tissues, and is fused to a modified form of the estrogen receptor (Ert2). This receptor cannot bind to estrogen, but instead has an affinity for the estrogen antagonist tamoxifen. The ubiquitously-expressed Ert2-Cre protein is retained within the cytoplasm, and is

therefore denied access to DNA. However, upon administration of tamoxifen to mice, Ert2-Cre is translocated to the nucleus where it has access to nuclear DNA and is able to cut and splice loxP sites. Adult homozygous *rasa1*$^{fl/fl}$ mice with or without the Ub-Ert2-Cre transgene were thus given injections of tamoxifen on two consecutive days. After 1 week, mice were sacrificed and expression of RASA1 in different tissues was assessed by Western blotting as before (Figure 8). As shown, substantial deletion of RASA1 was observed in thymus, spleen, LN and kidney of *rasa1*$^{fl/fl}$ *Ub-Ert2-Cre* Tg mice following tamoxifen treatment. Slightly less deletion was observed in lung and brain. However, in subsequent experiments we determined that, when given two repeat tamoxifen injections on consecutive days 1 week after the initial injections, RASA1 expression was almost completely lost in these tissues (as determined in Western blotting experiments performed 1 week later – not shown). Therefore, these mice are useful for study of the influence of induced loss of RASA1 expression in a variety of tissues of adult mice. Up to 6 weeks after tamoxifen treatment, mice remain healthy and show no obvious morphological signs of disease. After this time, however, these mice begin to die of a dysfunction of the lymphatic system. This phenomenon is described in detail in Chapter 4.

2.7 Absence of truncated RASA1 protein

Importantly, in all tissues to which Cre has been targeted, lower molecular mass forms of RASA1 have not been identified in Western blots (Figure 8).

Absence of these forms cannot be explained by simple loss of antibody epitopes from truncated RASA1 protein(s) since antibodies used in Western blot experiments were generated against NH_2-terminal SH2 and SH3 domains. Thus, deletion of exon 18 appears to result in a null *rasa1* allele with complete loss of RASA1 expression. To examine if transcripts generated from the *rasa1* exon 18-deleted allele were of low abundance relative to transcripts generated from the wild type *rasa1* allele, we performed RT-PCR analyses upon thymus RNA from *rasa1*$^{fl/+}$ mice with a pLCK-Cre transgene (Figure 9). Based upon analysis of protein expression in homozygote *rasa1*$^{fl/fl}$ *pLCK-Cre* Tg mice (Figure 8), almost 100% deletion of the floxed allele is expected in the heterozygotes. Using a forward primer located in exon 17 and reverse primers located in exons 19, 21, or 23, it was demonstrated that transcripts generated from the mutant allele are expressed much less abundantly than transcripts generated from the wild type allele in the same tissue (Figure 9). Furthermore, these analyses indicate that in mutant transcripts, exon 17 is spliced exclusively to exon 19 and not to other downstream exons. Results of RT-PCR reactions using a forward primer based in exon 13 with the same reverse primers concur with these conclusions (not shown). Low abundance of mutant transcripts is probably explained by nonsense-mediated RNA decay and is likely a major contributing factor to our inability to detect truncated lower molecular mass RASA1 forms in Western blots. Additionally, any lower molecular forms that are produced may be subject to rapid proteolytic degradation.

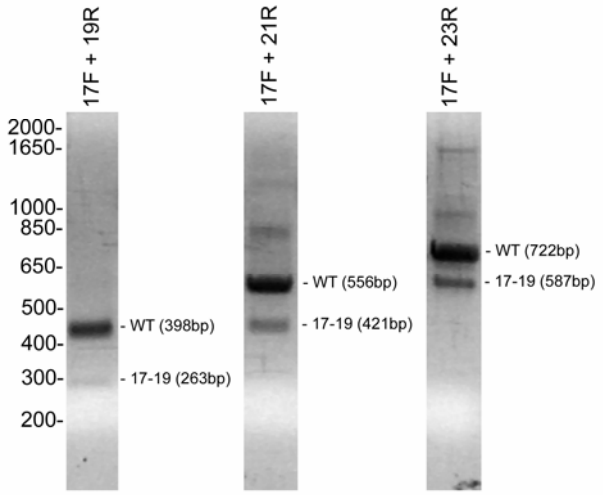

Figure 9: Relative abundance of wild type *rasa1* and *rasa1* exon 18-deleted transcripts in thymus. Total RNA from thymus of *pLCK-Cre* Tg heterozygote *rasa1*$^{fl/+}$ mice was analyzed by RT-PCR using a forward primer based in exon 17 and reverse primers based in exons 19, 21, or 23. PCR products generated from wild type and mutant *rasa1* transcripts are indicated. For each primer pair, the size of the smaller PCR product is consistent with an exon 17 to 19 splice of the mutant transcript. Note that in each case, the abundance of mutant PCR product is low compared with that of the wild type PCR product.

2.8 Materials and Methods

2.8.1 Generation of Conditional *rasa1* Knockout Mice

A *rasa1* targeting construct was assembled in p-loxP-2FRT-PGKneo (82). 5' and 3' arms and an inter-loxP region were generated by PCR from a C57BL/6 genomic *rasa1* BAC clone and were inserted into the EcoRI/KpnI, KpnI/SalI and XhoI sites of p-loxP-2FRT-PGKneo, respectively. Primers used for generation of PCR products were: 5'armF-5'-GCG CGA ATT CGC GGC CGC TTA GTC TTT CAG GCA TTT TAT AGC-3', 5'armR-5'-GCG CGG TAC CGA ATG CTT ATT TAC CAG GAG TGA C-3'; inter-loxPF-5'-GCG CGG TAC CAG ATC TAT AAC TTC GTA TAA TGT ATG CTA TAC GAA GTT ATA AAT ATT TGA GCC TAT

GAG GAC CA-3', inter-loxPR- 5'-GCG CGT CGA CCA TAT CCA ACT TCA CAT GAT GTG C-3'; 3'armF-5'-GCG CCT CGA GGA ATT TCC CAC ATG GAT AAT GCC A-3', 3'armR-5'-GCG CCT CGA GAT ATG TTG TCA TGT AAG ATC AAT TTC A-3'. The resulting targeting construct contained a 5' loxP site inserted in intron 17, a 3' loxP site and FRT-flanked NeoR cassette inserted in intron 18 (~900 bp downstream from the 3' loxP site) and 3.5 kbp of upstream and 2.7 kbp of downstream flanking sequence (Figure 6). Absence of PCR-induced errors was verified by DNA sequencing. The construct was linearized with NotI and electroporated into W4 ES cells of 129/Sv origin. Neomycin-resistant clones were analyzed by Southern blotting for correct targeting. 5' and 3' probes used in Southern blotting experiments were generated by PCR from the genomic *rasa1* BAC clone using the following primers: 5'probeF-5'-GCA AAA TTT CAT CTA GGA-3', 5'probeR-5'-CCT CAA TGA ACA AAC TTT-3'; 3'probeF- 5'-GAA TGT CTA ATA GTG CCC-3', 3'probeR-5'-GAT TAC TTA CAA TAA TTA-3'. Of several identified euploid correctly-targeted clones, two were injected into C57BL/6J X (C57BL/6J X DBA/2) blastocysts to generate chimeric mice, which were then bred with C57BL/6J mice to achieve germline transmission of the targeted allele. As determined by Southern blotting of tail DNA, germline transmission was achieved for both clones. Mice that had inherited the targeted allele from one of the ES cell clones (clone no.5041) were bred with C57BL/6 actin-promoter-driven Flp Tg mice to delete the NeoR cassette (77). Mice were then intercrossed to generate wild type, heterozygote or homozygote *rasa1*$^{fl/fl}$ mice (Figure 7). Genotyping for *rasa1* alleles was performed by PCR of tail DNA using the

following primers: F-5'-CAG TTT GTT CAT CAT GCT TTG-3', R-5'-GAA GTT TGA CTT TGG TTG CTG-3'. Alternatively, *rasa1*$^{fl/fl}$ mice were crossed with C57BL/6 mice carrying a Cre transgene driven by the proximal Lck promoter (Taconic) or an inducible Ert2-Cre transgene driven by a ubiquitin promoter (79, 81). Heterozygote *rasa1*$^{fl/+}$ Cre-positive progeny from these crosses were then backcrossed with heterozygote *rasa1*$^{fl/+}$ mice to generate wild type or homozygote *rasa1*$^{fl/fl}$ mice either not expressing or expressing Cre transgenes (Figure 8). All experiments performed upon mice were in compliance with University of Michigan guidelines and were approved by the University Committee on the Use and Care of Animals.

2.8.2 Tamoxifen Administration

Two-month-old homozygous *rasa1*$^{fl/fl}$ mice with and without *Ub-Ert2-Cre* transgenes were administered tamoxifen (MP biochemicals) to induce nuclear translocation of the Ert2-Cre protein. On the basis of an earlier study, in which the same *Ub-Ert2-Cre* transgene was utilized, a dose of 0.2 mg/g body weight of tamoxifen was chosen (81). Tamoxifen was injected intraperitoneally in 200 μl of autoclaved corn oil (Sigma). Mice were given two injections on consecutive days. Seven days later mice were sacrificed for analysis.

2.8.3 Western Blotting

Lysates of different organs of 2-month-old pLCK-Cre Tg wild type and homozygous *rasa1*$^{fl/fl}$ mice and from tamoxifen-treated *rasa1*$^{fl/fl}$ mice with and

without *Ub-Ert2-Cre* transgenes were prepared by dounce homogenization in 1% NP-40 lysis buffer. Expression of RASA1 in lysates was determined by Western blotting using an antibody generated against the SH2 and SH3 domains of RASA1 (Millipore). Blots were stripped and reprobed with actin or GAPDH antibodies to demonstrate equivalent protein loading.

2.8.4 RT-PCR

Total RNA was prepared from thymus of pLCK-Cre Tg heterozygote *rasa1*$^{fl/+}$ mice with Trizol reagent (Gibco) and reverse-transcribed using a Superscript II kit (Invitrogen) and random primers. cDNA was amplified by PCR using a forward primer based in exon 17 and reverse primers based in exons 19, 21, and 23. Primer sequences are as follows: 17F-5'-CAA AAG GAA CTT CAT GTC GTC-3', 19R-5'-GGA AGT ATT TCT GAA GCC ATG-3', 21R-5'-CTG AGA TGA TAT TAA ACA TCC-3', 23R-5'-CCC AAG TTC ATC TAA AAA CAT-3'.

Chapter 3

Conditional deletion of RASA1 in T cells reveals its role as a regulator of T cell development and function

3.1 Abstract

TCR-induced activation of the Ras small GTP-binding protein is necessary for normal T cell development and function. However, how Ras is inactivated in T cells following TCR ligation is poorly understood. Here, we used conditional gene targeted mice to investigate the possibility that the prototypical RasGAP RASA1 is essential for the inactivation of Ras in T cells. T cell-specific RASA1-deficient mice showed evidence of increased positive selection in the thymus that was associated with augmented Ras/MAPK signal transduction. In the periphery, T cell-specific RASA1-deficient mice exhibited a peripheral CD8+ T cell lymphopenia and an increased percentage of T cells that expressed the CD44 memory marker. Most importantly, naïve RASA1-deficient CD4+ and CD8+ T cells synthesized markedly elevated amounts of cytokines in response to peptide-MHC stimulation. Furthermore, this hyperresponsiveness was accompanied by augmented peptide-MHC induced activation of the Ras/MAPK pathway. These findings point to an important non-redundant role for RASA1 as

a negative-feedback regulator of TCR-induced Ras activation that controls T cell development, homeostasis and activation.

3.2 Introduction

Ras is a small G protein, tethered to the inner leaflet of the cell membrane that cycles between inactive GDP-bound and active GTP-bound states (2). In its GTP-bound state, Ras triggers activation of downstream signaling pathways, such as the MAPK signaling pathway that regulates cell growth and differentiation (9). In the T cell lineage, numerous studies have illustrated the importance of Ras and MAPK for T cell development and function. In the thymus, Ras/MAPK signal transduction is necessary for pre-TCR-induced transition of CD4-CD8- DN thymocytes into CD4+CD8+ DP thymocytes (56, 58). Furthermore, the Ras/MAPK pathway is essential for TCR-mediated positive selection of DP cells resulting in their maturation into CD4+ or CD8+ SP T cells (56, 83, 84). In peripheral T cells, TCR-induced activation of the Ras/MAPK pathway is necessary for T cell activation and differentiation (59, 60). Active Ras also serves to activate PI3K, which in turn activates the serine kinase AKT (6, 8). This pathway activates the transcription factor NFκB, which can mediate cell survival and death by apoptosis. Through these different signaling pathways, Ras plays a critical role in T cell activation, survival, and differentiation.

The mechanism by which the TCR activates Ras has been well studied and involves mobilization of the GEFs, mammalian SOS and RasGRP1, to cell membranes (40-42). These GEFs activate Ras by ejecting GDP from the Ras

guanine nucleotide-binding pocket, thereby permitting Ras to bind GTP, which is present in higher concentrations than GDP in the cytosol. Inactivation of Ras involves Ras-mediated hydrolysis of GTP to GDP. However, Ras has only weak GTP-ase activity and, therefore, RasGAPs are required for efficient inactivation of Ras (12, 13). Through physical interaction, RasGAPs increase the ability of Ras to hydrolyze GTP by several orders of magnitude.

At least 10 different RasGAPs have now been identified in mammals (12). However, with the exception of NF1, which of these RasGAPs inactivate Ras in T cells has been poorly studied. Non-conditional disruption of the *nf1* gene in mice causes embryonic lethality associated with cardiovascular and other developmental defects (67). Therefore, to study the role of NF1 in T cells, NF1-deficient hematopoietic stem cells (HSC) were adoptively transferred into adult T cell-deficient recipients (68). Compared to mice receiving wild type HSC, numbers of thymocytes and peripheral T cells were increased in recipient mice. Furthermore, T cells from these mice showed elevated levels of Ras-GTP prior to but not subsequent to TCR stimulation. This finding has led to the conclusion that NF1 negatively regulates Ras activation in quiescent T cells but that other RasGAPs negatively regulate Ras once Ras has been activated by TCR signaling.

One other RasGAP that has been implicated as a regulator of Ras in T cells is RASA1 (85). Non-conditional RASA1-deficient mice succumb *in utero*, probably as a result of defective vascular development (32). However, owing to the early embryonic lethality in this model, it has not been possible to perform

HSC adoptive transfer experiments to assess the importance of RASA1 in the T cell lineage. Therefore, to address this question, we generated T cell-specific RASA1-deficient mice. Studies of these mice have revealed that RASA1 is indeed an important negative-regulator of Ras in T cells that controls T cell development and function.

3.3 RASA1-deficient T cell development

We have reported previously the generation of mice that carry conditional (i.e. flanked by-loxP) null alleles of rasa1 (*rasa1*$^{fl/fl}$ mice) (Chapter 2). To delete RASA1 in the T cell lineage, mice were crossed with Tg mice that express pLCK-Cre (79). In these mice, Cre is expressed from the DN3 (CD44-CD25+) stage of thymocyte development onward. We first examined the influence of RASA1 loss upon T cell development. For these experiments, we determined ratios of DN, DP and SP cells in thymi of *rasa1*$^{fl/fl}$ *pLCK-Cre* mice and littermate control *rasa1*$^{fl/fl}$ mice by flow cytometry (Figure 10). The percentage representation of these subsets was found to be normal in *rasa1*$^{fl/fl}$ *pLCK-Cre* mice as was the ratio of DN3 (CD44-CD25+) to DN4 (CD44-CD25-) cells. Total numbers of thymocytes were also unaltered in *rasa1*$^{fl/fl}$ *pLCK-Cre* mice compared to controls (not shown). These findings indicated that RASA1 might not be required for normal pre-TCR signaling or positive selection of thymocytes. Apparent lack of a thymic phenotype in these mice could not be explained by inefficient disruption of the *rasa1* gene as RASA1 protein was undetectable by Western blotting of cell lysates prepared from whole thymus (Figure 10).

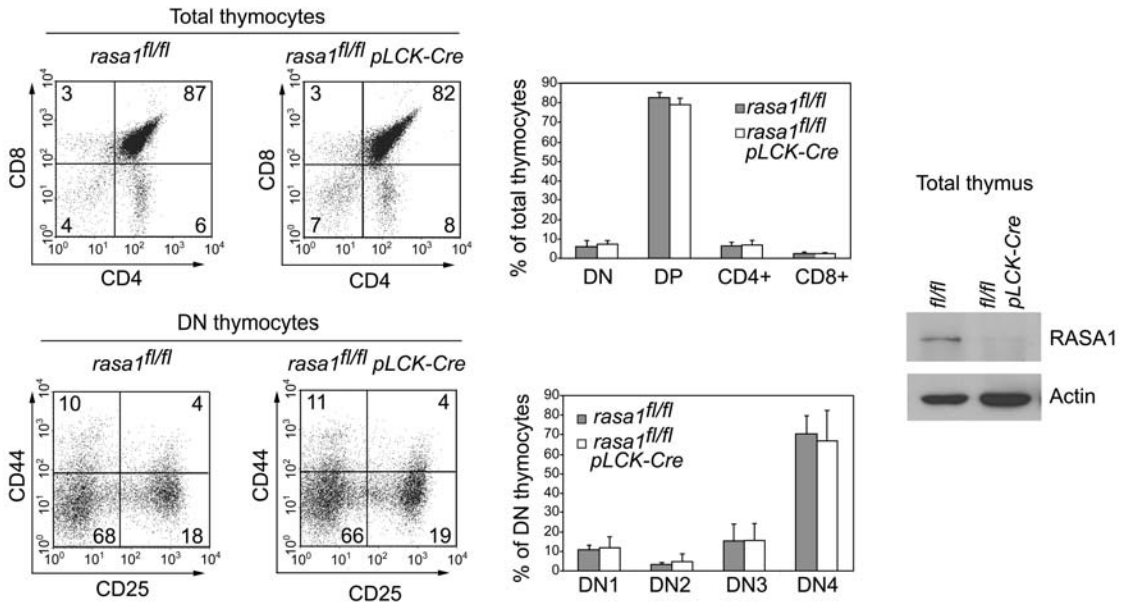

Figure 10: T cell development in T cell-specific RASA1-deficient mice. Cell surface expression of CD4, CD8, CD44 and CD25 upon thymocytes of *rasa1*$^{fl/fl}$ and *rasa1*$^{fl/fl}$ *pLCK-Cre* mice was analyzed by flow cytometry. Two-color plots show expression of CD4 and CD8 upon whole thymocytes or of CD44 and CD25 expression upon DN thymocytes. Bar charts show mean percentage + 1 SD of DN, DP, CD4 and CD8 SP among total thymocytes or DN1 (CD44+CD25-), DN2 (CD44+CD25+), DN3 (CD44-CD25+) and DN4 (CD44-CD25-) among total DN thymocytes as determined from replicate experiments (*fl/fl*, n=8; *fl/fl pLCK-Cre*, n=6). At right is a representative Western blot showing expression of RASA1 in whole thymocytes of littermate *rasa1*$^{fl/fl}$ and *rasa1*$^{fl/fl}$ *pLCK-Cre* mice. Blots were stripped and reprobed with an actin antibody to demonstrate equivalent protein loading.

3.4 Positive selection in Tg TCR mice

We next examined the influence of RASA1 loss upon T cell development in TCR Tg mice in which the majority of T cells express a TCR of a singular specificity. It was reasoned that a role for RASA1 in T cell development might be revealed in these mice that would not be readily apparent in a polyclonal setting. For this purpose, we generated HY TCR Tg and AND TCR Tg *rasa1*$^{fl/fl}$ and *rasa1*$^{fl/fl}$ *pLCK-Cre* mice. The HY TCR recognizes a male-specific HY peptide in the context of the MHC class I molecule, H-2D^{b} (86). In female H-2^{b} HY TCR Tg

mice, HY TCR Tg DP cells are positively-selected upon recognition of H-2D^b and mature into CD8+ SP T cells. The AND TCR has specificity for pigeon cytochrome c (PCC) peptide 88-104 in the context of the MHC class II molecule I-E^k (87). In H-2^b mice, AND TCR Tg DP cells are positively-selected on the MHC class II molecule I-A^b, and mature into CD4+ SP T cells. Use of these two different TCR Tg models on an H-2^b background, therefore, affords an opportunity to examine positive selection upon MHC class I and class II at a clonal level. Specifically, we examined the ratio of SP to DP thymocytes in *rasa1*$^{fl/fl}$ and *rasa1*$^{fl/fl}$ *pLCK-Cre* TCR Tg mice as an indicator of the efficiency of positive selection (Figure 11A). In female *rasa1*$^{fl/fl}$ *pLCK-Cre* HY TCR Tg mice, the ratio of CD8+ SP to DP cells in thymus was the same as that observed in *rasa1*$^{fl/fl}$ HY TCR Tg mice, indicating that positive selection proceeds normally in the absence of RASA1 in this model. By contrast, in *rasa1*$^{fl/fl}$ *pLCK-Cre* AND TCR Tg mice, the ratio of CD4+ SP to DP cells in thymus was increased relative to that observed in *rasa1*$^{fl/fl}$ AND TCR Tg mice (total thymic cellularity was unaltered by the loss of RASA1 in both TCR Tg models). This finding is consistent with the idea that positive selection in AND TCR Tg mice is more efficient in the absence of RASA1. Based upon this observation, we next asked if there was evidence of increased activation of the Ras/MAPK pathway in DP thymocytes of *rasa1*$^{fl/fl}$ *pLCK-Cre* AND TCR Tg mice. To examine this, we performed intracellular staining experiments on AND TCR Tg thymocytes using a phospho-specific MAPK mAb to identify activated forms of MAPK (Figure 11B). Flow cytometric analysis of stained cells revealed that a larger percentage of DP thymocytes in

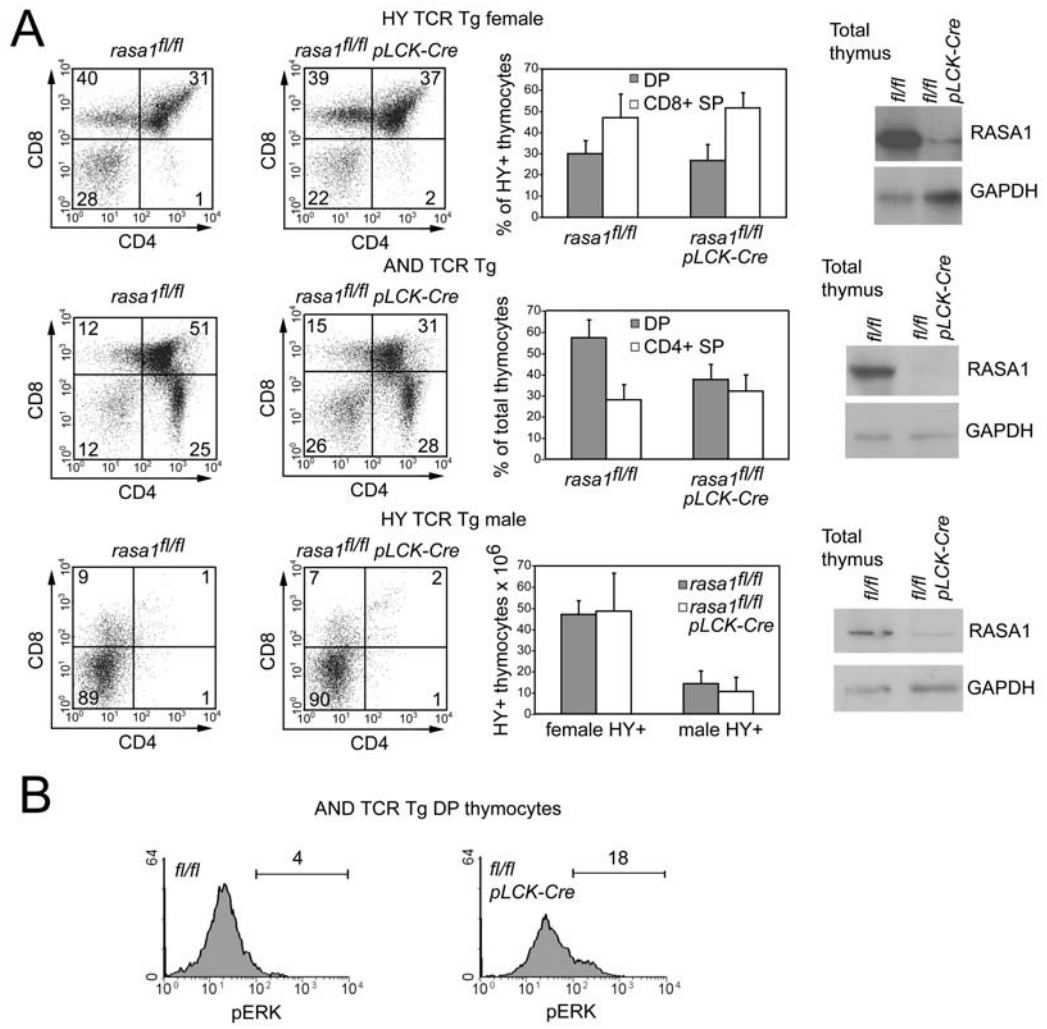

Figure 11: T cell development in TCR Tg T cell-specific RASA1-deficient mice. (A) Expression of CD4 and CD8 upon thymocytes of female and male HY TCR Tg and AND TCR Tg *rasa1*$^{fl/fl}$ and *rasa1*$^{fl/fl}$ *pLCK-Cre* mice was determined by flow cytometry. At left are shown representative two-color plots of littermate mice. For HY TCR Tg mice, plots depict T3.70hi HY TCR+ gated thymocytes. Bar charts show mean percentage + 1 SD of DP and CD8+ SP cells among HY TCR+ thymocytes for female HY TCR Tg mice (*fl/fl*, n=7; *fl/fl pLCK-Cre*, n=5), mean percentage + 1SD of DP and CD4 SP cells among total thymocytes for AND TCR Tg mice (*fl/fl*, n=8; *fl/fl pLCK-Cre*, n=9) and total numbers + 1 SD of HY TCR+ thymocytes for female and male HY TCR Tg mice (female *fl/fl*, n=8; female *fl/fl pLCK-Cre*, n=5; male *fl/fl*, n=6; male *fl/fl pLCK-Cre*, n=5). At right are shown representative Western blots of RASA1 expression in whole thymi of the respective Tg mice. Blots were reprobed with a GAPDH antibody. **(B)** Thymocytes from littermate *rasa1*$^{fl/fl}$ and *rasa1*$^{fl/fl}$ *pLCK-Cre* AND TCR Tg mice were stained with CD4, CD8 and pERK antibodies and analyzed by flow cytometry. Shown are histogram plots of pERK staining gated upon DP cells.

rasa1$^{fl/fl}$ *pLCK-Cre* AND TCR Tg mice expressed activated forms of MAPK compared to DP thymocytes in *rasa1*$^{fl/fl}$ AND TCR Tg mice. This increased activation of MAPK is consistent with and presumably accounts for the increased positive selection in the absence of RASA1 in AND TCR Tg mice.

3.5 Negative selection Tg TCR mice

In male HY TCR Tg male mice, expression of the HY peptide upon thymic stromal cells results in clonal deletion of HY TCR-expressing DP cells, i.e. negative selection (86). Therefore, we compared thymi of male *rasa1*$^{fl/fl}$ *pLCK-Cre* and *rasa1*$^{fl/fl}$ HY TCR Tg mice to determine if there was any influence of RASA1 loss upon negative selection (Figure 11 A). However, thymi from both types of male mice showed the same complete loss of DP cells and total reductions in cellularity compared to female HY TCR Tg mice. We conclude, therefore, that expression of RASA1 is not necessary for thymic negative selection. Moreover, there are no signs of autoimmune disease development (lymphadenopathy, splenomegaly, vasculitis, etc.) in T cell specific RASA1- deficient mice, consistent with the notion that negative selection is intact in these animals.

3.6 Positive selection in a competitive environment

We next sought evidence that the increased positive selection observed in AND TCR Tg mice in the absence of RASA1 was more generally applicable to

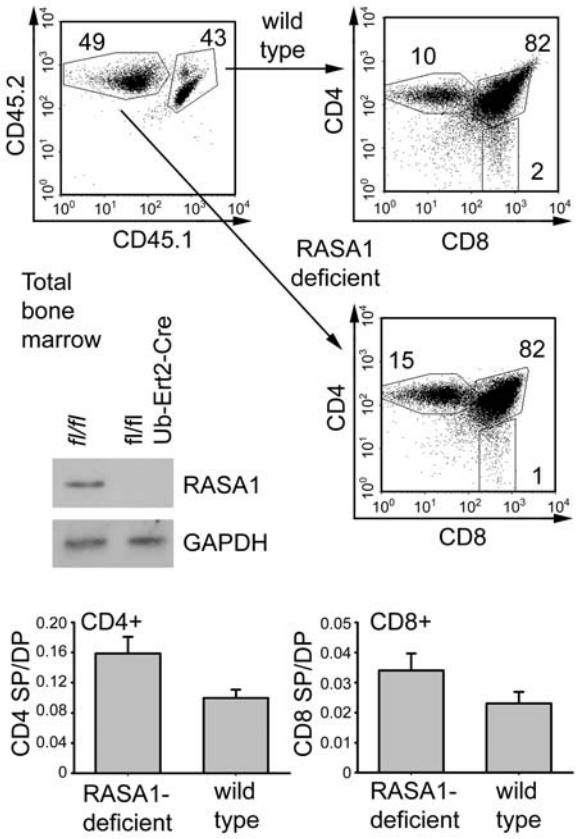

Figure 12: Development of RASA1-deficient T cells in a competitive thymic environment. Bone marrow from wild type (CD45.1/CD45.2) and *rasa1*$^{fl/fl}$ *Ub-Ert2-Cre* mice (CD45.2) treated with tamoxifen 3 weeks previously was adoptively transferred to sublethaly-irradiated wild type (CD45.1) mice. Loss of RASA1 expression in *rasa1*$^{fl/fl}$ *Ub-Ert2-Cre* bone marrow following tamoxifen treatment was confirmed by Western blotting. After 2 months, thymi were stained with CD45.1, CD45.2, CD4 and CD8 mAb and examined by flow cytometry. Shown are representative two-color plots of CD45.1/CD45.2 expression and CD4/CD8 expression upon gated wild type and RASA1-deficient cells that have developed in the same thymus. Bar charts show the mean CD4+ SP/DP or CD8+ SP/DP ratio + 1 SD for wild type and RASA1-deleted thymocytes as determined in replicate experiments (total number of recipient mice = 6). Differences between wild type and RASA1-deficient thymocytes are statistically significant ($p<0.0082$ for the CD4+ SP/DP ratio and $p<0.0133$ for the CD8+ SP/DP ratio, as determined using a paired Student's two sample t-test).

MHC class II-restricted T cells. For this purpose, we performed competitive bone marrow adoptive transfer experiments in which a 50:50 mix of wild type and RASA1-deficient bone marrow was injected into lethally-irradiated

wild type mice. RASA1-deficient bone marrow was obtained from *rasa1*$^{fl/fl}$ *Ub-Ert2-Cre* mice that had been treated with tamoxifen 3 weeks previously (Figure 12). Six weeks after adoptive transfer, thymi were harvested from mice and T cell development was analyzed by flow cytometry. Developing T cells derived from wild type and RASA1-deficient bone marrow were readily distinguished by staining for CD45 allelic markers. In these experiments, the CD4+ SP/DP ratio was consistently greater for thymocytes derived from RASA1-deficient bone marrow than for thymocytes derived from wild type bone marrow (Figure 12). Thus, in a competitive environment, a role for RASA1 as a negative-regulator of positive section of CD4+ cells is readily revealed in a non-TCR Tg setting. Interestingly, in the same thymi, the CD8+ SP/DP ratio was also found to be greater for RASA1-deficient thymocytes compared to wild type thymocytes (on average), albeit that the statistical significance of this difference was less than that observed for the CD4+ SP/DP ratio (Figure 12). Therefore, RASA1 also appears to regulate the positive selection of CD8+ T cells in a competitive environment.

3.7 Reduced numbers of peripheral T cells with increased CD44 expression in T cell-specific RASA1-deficient mice

In the peripheral lymphoid organs of non-TCR Tg T cell-specific RASA1-deficient mice, we observed reduced proportions and numbers of T cells (Figure 13 A). This was most apparent for CD8+ T cells, which were reduced in

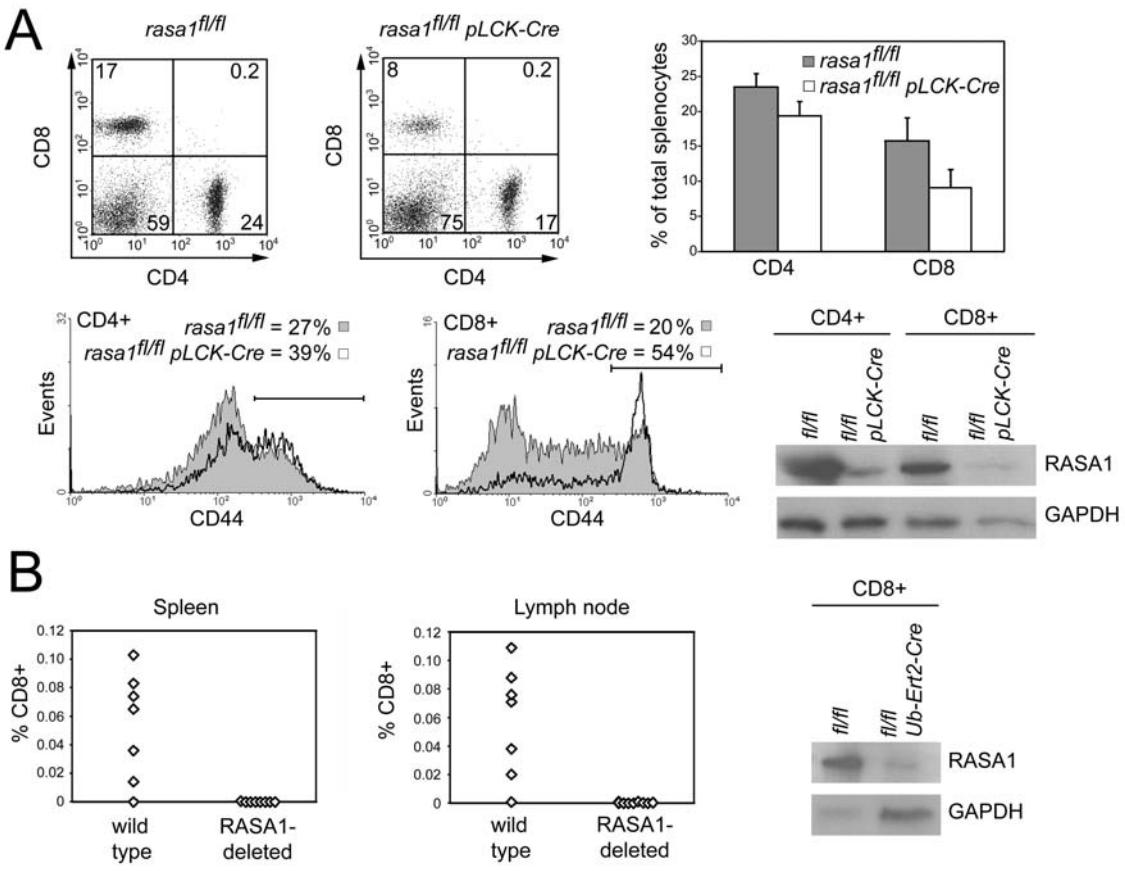

Figure 13: Reduced survival of CD8+ T cells in peripheral lymphoid organs of T cell specific RASA1-deficient mice. (A) Two-color flow cytometry plots depict CD4/CD8 expression upon splenocytes of representative littermate *rasa1*$^{fl/fl}$ and *rasa1*$^{fl/fl}$ *LCK-Cre* mice. The mean percentage + 1 SD of CD4+ and CD8+ T cells in spleen as determined in replicate experiments is shown at top right (*fl/fl*, n=7; *fl/fl pLCK-Cre*, n=6). Differences in the mean percentage of CD4+ and CD8+ T cells between mice are statistically significant ($p<0.0023$ for CD4+ T cells and $p<0.0013$ for CD8+ T cells using a Student's two sample t-test). Histograms show expression of the CD44 memory cell marker upon gated CD4+ and CD8+ T cells from representative littermate *rasa1*$^{fl/fl}$ and *rasa1*$^{fl/fl}$ *pLCKCre* mice. Western blots show expression of RASA1 in purified splenic CD4+ and CD8+ T cells from littermate *rasa1*$^{fl/fl}$ and *rasa1*$^{fl/fl}$ *LCK-Cre* mice. **(B)** CD8+ T cells were purified from spleen and LN of wild type and *rasa1*$^{fl/fl}$ *Ub-Ert2-Cre* mice treated with tamoxifen 5 weeks beforehand. Cells were CFSE-labeled and injected into tail veins of wild type recipient mice. After 2 weeks, CFSE+ cells were identified in spleen and LN of recipient mice by flow cytometry. Plots show the percentage of donor CD8+ T cells among total CD8+ T cells in each organ. Each point represents a single recipient mouse that received the indicated type of CD8+ T cell. Loss of RASA1 in purified CD8+ T cells from *rasa1*$^{fl/fl}$ *Ub-Ert2-Cre* mice treated with tamoxifen 5 weeks previously was confirmed by Western blotting.

number by as much as 50%. Further analysis of the RASA1-deficient T cells revealed that an increased percentage expressed the CD44 marker of memory T cells. Neither CD4+ nor CD8+ SP T cells express CD44 in the thymus of T cell-specific RASA1-deficient mice (similar to control mice); hence, the increased expression of CD44 must arise in the periphery. Identical results were obtained with *rasa1*$^{fl/fl}$ *Ub-Ert2-Cre* mice treated with tamoxifen. Thus, 3 months after tamoxifen administration, *rasa1*$^{fl/fl}$ *Ub-Ert2-Cre* mice showed reduced numbers of T cells (primarily CD8+) and an increased percentage of T cells that expressed CD44 relative to tamoxifen-treated *rasa1*$^{fl/fl}$ mice (not shown).

3.8 RASA1-deficient T cell survival

Long term survival of naïve CD44 low T cells in immunocompetent hosts depends upon TCR recognition of self MHC (88, 89). Since RASA1 has been implicated as an anti-apoptotic factor in fibroblasts (in a manner that is independent of its GAP activity), we speculated that reduced numbers of T cells with increased levels of CD44 expression in T cell-specific RASA1-deficient mice could potentially be explained by a role for RASA1 in naïve T cell survival specifically (30). To examine this, we purified CD8+ T cells from LN and spleen of wild type and *rasa1*$^{fl/fl}$ *Ub-Ert2-Cre* mice that had been treated with tamoxifen 5 weeks previously. Cells were then labeled with the fluorescent dye CFSE, and injected into the tail veins of wild type recipient mice. After 2 weeks, the percentage representation of donor CD8+ T cells among total CD8+ T cells in LN and spleen was determined by flow cytometry (Figure 13 B). As shown, wild type

CD8+ T cells were detected in spleens and LN in 6 out of 7 recipient mice. By contrast, RASA1-deficient T cells were not detected in any of 8 recipients. Notably, neither CD44-low naive nor CD44+ memory RASA1-deficient T cells were found in recipients, whereas both naïve and memory T cells from wild type mice were detected in recipients and in the same ratio that they were represented prior to transfer. The possibility that the disappearance of the RASA1-deficient CFSE labeled cells is due to excessive proliferation, and hence dilution of the CFSE dye, can be excluded as RASA1-deficient CFSE labeled cells were present at 1 weeks post-injection, and showed no apparent proliferation (not shown). We conclude, therefore, that at least for CD8+ T cells, RASA1 regulates the long term survival of both naïve and memory subsets. An increased percentage of T cells with a memory phenotype in T cell-specific RASA1-deficient mice could potentially be explained by other factors such as increased responsiveness of T cells to antigen (see below) and/or homeostatic proliferation to correct a peripheral T cell number deficit.

3.9 Enhanced cytokine synthesis by naïve RASA1-deficient T cells

To assess the influence of RASA1 loss upon T cell cytokine synthesis, we used TCR Tg mice in order to examine responses induced by physiological MHC-peptide ligands rather than surrogate TCR complex antibodies. Given the increased frequency of CD44+ memory phenotype T cells in non-TCR Tg mice, however, we were careful to focus upon responses of naïve T cells only. In female HY TCR Tg mice, HY TCR+ peripheral T cells do not express CD44,

which has been attributed, at least in part, to an inability of these cells to undergo homeostatic proliferation (41, 90). Likewise, HY TCR+ T cells in *rasa1*$^{fl/fl}$ *pLCK-Cre* HY TCR Tg mice did not express CD44, similar to HY TCR+ T cells in *rasa1*$^{fl/fl}$ HY TCR Tg mice (not shown). Therefore, to examine the effect of RASA1 loss in the HY TCR Tg system, purified CD8+ T cells from female mice were stimulated directly with female H-2^{b} APC in the absence or presence of HY peptide (Figure 14 A). As shown, RASA1-deficient T cells secreted much larger quantities of the cytokines IL-2 and IFN-γ in response to peptide-MHC stimulation over a range of peptide concentrations. These findings show that RASA1 functions as an important non-redundant negative-regulator of cytokine synthesis in naïve CD8 T cells.

Unlike HY TCR Tg T cells, peripheral T cells from AND TCR Tg mice are able to express CD44. Furthermore, a larger percentage of peripheral T cells were found to express CD44 in *rasa1*$^{fl/fl}$ *pLCK-Cre* AND TCR Tg mice compared to *rasa1*$^{fl/fl}$ AND TCR Tg mice (not shown). Therefore, to examine the effect of RASA1 loss in the AND TCR Tg system, we used purified CD4+CD44-low naïve T cells as responders. Cells were stimulated with I-E^{k} APC in the absence or presence of PCC peptide (Figure 14 A). Again, the RASA1-deficient T cells synthesized substantially larger quantities of IL-2 and IFN-γ in response to peptide-MHC stimulation over a range of peptide concentrations. Thus, RASA1 also appears to function as an important negative regulator of cytokine synthesis in naive CD4+ T cells.

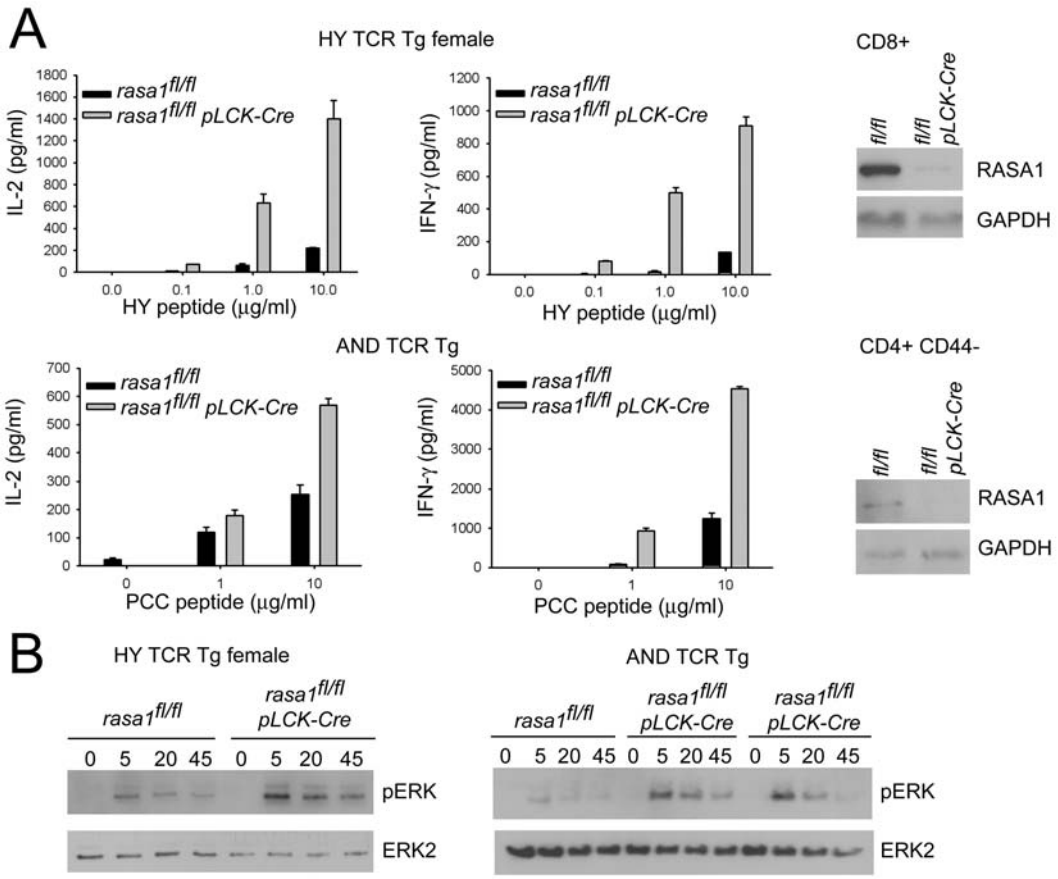

Figure 14: Peptide-MHC-induced cytokine synthesis and Ras/MAPK activation in RASA1-deficient T cells. (A) CD8+ and CD4+CD44- naïve T cells were purified from spleens of female HY TCR Tg and AND TCR Tg mice (littermate *rasa1*$^{fl/fl}$ and *rasa1*$^{fl/fl}$ *pLCK-Cre*) and stimulated with female H-2^{b} APC plus HY peptide or I-E^{k} APC plus PCC peptide respectively. Concentrations of IL-2 and IFN-γ in culture supernatants were determined by ELISA after 48 h. Mean cytokine concentrations + 1SD of triplicate determinations are depicted for each peptide dose. Experiments shown are representative of at least three performed. Western blots show expression of RASA1 in purified CD8+ and CD4+CD44- T cell populations from respective HY TCR Tg and AND TCR Tg mice. **(B)** The same purified naïve T cell populations in (A) were stimulated with the same peptide-pulsed (10 μg/ml) APC for the indicated times in min. Cells were then lysed and activation of the Ras/MAPK pathway was determined by Western blotting using a phospho-specific ERK antibody. Blots were reprobed with an ERK2 antibody to ascertain that equivalent quantities of ERK were loaded on gels. In the depicted AND TCR Tg experiment, results from one *rasa1*$^{fl/fl}$ and two independent *rasa1*$^{fl/fl}$ *LCK-Cre* mice are shown. The same results have been obtained in 3 independent experiments for each type of TCR Tg mouse.

3.10 Enhanced Ras/MAPK signaling in RASA1-deficient T cells

To determine if increased cytokine synthesis by RASA1-deficient T cells is accompanied by increased activation of the Ras/MAPK signaling pathway, naïve RASA1-deficient and -sufficient HY and AND TCR Tg T cells were stimulated with cognate peptide-MHC ligands as above. Activation of the Ras/MAPK pathway was then assessed by Western blotting to detect phosphorylated forms of MAPK (Figure 14 B). In unstimulated RASA1-deficient T cells no increased activation of MAPK was detected. However, 5 min after initiation of the peptide-MHC induced response, RASA1-deficient HY and AND TCR Tg naïve T cells both showed markedly increased activation of MAPK. Thereafter, RASA1-deficient T cells also showed increased activation of MAPK relative to control T cells, although levels of activation were decreased relative to their peak at 5 min. These findings are significant in that they identify RASA1 as a negative-feedback regulator of peptide-MHC-induced Ras/MAPK activation in T cells rather than a constitutive negative-regulator of this pathway in this cell type. Loss of this negative-regulatory function presumably accounts for the increased peptide-MHC-induced cytokine synthesis of RASA1-deficient T cells.

3.11 Generation of RASA1-deficient B cells and myeloid cells

To determine the role of RASA1 in other immune cell types, we generated mouse models in which the *rasa1*$^{fl/fl}$ mice were crossed with mice expressing other immunocyte-specific forms of Cre. By crossing the *rasa1*$^{fl/fl}$ mice with mice expressing CD19-Cre (80) or LysM-Cre (78), we were able to specifically delete

RASA1 protein expression from B cells or myeloid cells, respectively. Comprehensive analysis of *rasa1*$^{fl/fl}$ *CD19-Cre* mice and *rasa1*$^{fl/fl}$ *LysM-Cre* mice indicates that RASA1 is dispensable for the normal functioning of B cells and myeloid cells. In *rasa1*$^{fl/fl}$ *CD19-Cre* mice, no defects were observed in B cell development, numbers, or ratios of B cell subsets in secondary lymphoid organs. B cell proliferation, survival and an ability of B cells to mount antibody responses and class switch in response to antigen challenge *in vivo* were also unchanged (not shown). In *rasa1*$^{fl/fl}$ *LysM-Cre* Tg mice, no defects in numbers and ratios of myeloid subsets in bone marrow, secondary lymphoid organs and peripheral non-lymphoid tissues were observed, and an ability of macrophages to engage in phagocytosis and secrete cytokines and anti-microbial factors in response to inflammatory stimuli was unaltered (not shown).

3.12 Discussion

In summary, we show here using conditional gene-targeted mice, that RASA1 is an essential negative-feedback regulator of TCR-induced activation of Ras that controls T cell development and function. The precise mechanisms by which RASA1 is targeted to Ras during TCR signaling and how RASA1 might cooperate with NF1 to control Ras activation in T cells deserve further study. It is likely that there are other RasGAPs, distinct from RASA1, that function in T cells, as the increased amount of phospho-MAPK observed in peptide-stimulated *rasa1*$^{fl/fl}$ *pLCK-Cre* TCR Tg T cells eventually returns to nearly baseline levels (Figure 14B). To study the potential synergy between RASA1 and NF1 in T cell

development and function, we have crossed *rasa1*$^{fl/fl}$ *pLCK-Cre* mice with mice expressing a floxed NF1 allele (91). The resulting *rasa1*$^{fl/fl}$ *nf1*$^{fl/fl}$ *pLCK-Cre* mice will express neither RASA1 nor NF1 in T cells, and will allow us to determine if there is an exacerbated T cell phenotype in the absence of both of these GAPs.

It is possible that the decrease in phospho-MAPK levels after stimulation in RASA1-deficient T cells is due to the action of MAPK-phosphatases, not a downregulation of Ras activity. In future experiments, we will directly measure Ras-GTP levels by ELISA or pulldown experiments with Raf1-RBD, a fragment of the Raf1 protein that recognizes the GTP-bound form of Ras. This will allow us to definitively determine if Ras activity is enhanced in RASA1-deficient T cells.

In addition, the question of whether all observed T cell phenotypes in *rasa1*$^{fl/fl}$ *pLCK-Cre* mice can be explained by aberrant activation of Ras or whether other molecular mechanisms are involved remains to be determined. Since RASA1 is known to be involved in a number of Ras-independent functions, the extent of involvement of Ras/MAPK signaling cannot be definitively determined. One way of determining if dysregulated Ras activation is solely responsible for the phenotype observed would be to generate *rasa1*$^{fl/fl}$ *pLCK-Cre mice* which also contain a bacterial artificial chromosome (BAC) that expresses a *rasa1* mutant gene in which the GAP domain is functionally deficient. This would allow the endogenous RASA1 protein to be expressed in all tissues except T cells, which would express only a form of RASA1 that is unable to catalyze GTPase activity in Ras. Using this system, we would expect that T cells expressing only the GAP domain-mutant RASA1 protein to have an increased

capacity to secrete cytokines that correlates with enhanced Ras/MAPK signaling, enhanced positive selection of thymocytes, and decreased survival of peripheral T cells, similar to RASA1-deficient T cells. These results would clearly demonstrate that dysregulated Ras/MAPK signaling is solely responsible for the observed phenotype. However, in the event that these animals do not display the expected phenotypes, or the phenotypes are reduced in severity, this result would suggest that RASA1 domains other than the GAP domain are involved. Which of the modular binding domains of RASA1 play a role in the development of the T cell phenotypes could be tested by generating BAC transgenes in which the modular binding domains (SH2-SH3-SH2) of RASA1 are inactivated. Expressing this mutant form of RASA1 in *rasa1*$^{fl/fl}$ *pLCK-Cre* mice would allow these mutants to be directly tested in their ability to modulate T cell development and function.

The question of whether increased cytokine synthesis observed in *rasa1*$^{fl/fl}$ *pLCK-Cre* T results in increased autoimmunity remains to be fully addressed. We have thus far not observed any signs of autoimmunity in *rasa1*$^{fl/fl}$ *pLCK-Cre* mice up to 1 year of age, such as diabetes, encephalitis, or hyperplasia of lymphoid organs. It is possible that the increased Ras/MAPK signaling in RASA1-deficient T cells and the resultant increase in cytokine secretion are balanced by decreased survival of these cells, and that auto-reactive T cells die before they are able to proliferate and cause disease.

Since RASA1-deficient T cells secrete greater amounts of cytokines after antigen stimulation, it might be possible that increased cytokine response could

produce an enhanced protection from pathogens. Testing this hypothesis would require infecting *rasa1*$^{fl/fl}$ or *rasa1*$^{fl/fl}$ *pLCK-Cre* mice with a model pathogen for which the T cell response has been shown to be important. The intracellular protozoan *Toxoplasma gondii* is known to elicit a strong Th1 response in mice, for example (92). By measuring the amounts of Th1 cytokines secreted by the infected mice, the amount of pathogen present in infected animals, and the rate of survival, it would be possible to determine the role of RASA1 in T cells responding to pathogen challenge. The model pathogen *Listeria monocytogenes*, the clearance of which is dependent on CD8+ cells, will also be used (93). CD8+ T cell numbers are more greatly affected by the absence of RASA1 than CD4+ T cells (Figure 13), and *Listeria* infection will allow us to specifically study this cell type in an infection model.

The lack of a phenotype in RASA1-deficient B cells and macrophages is surprising, considering that RASA1 is well expressed in these cell types (not shown). It is possible that there is a defect in one or both of these cell types which we have been unable to detect. Alternatively, the absence of RASA1 in these cells could be compensated by another, unidentified RasGAP that is not active in T cells.

3.13 Materials and Methods

3.13.1 Mice

The generation of *rasa1*$^{fl/fl}$ mice with and without *pLCK-Cre* and *Ub-Ert2-Cre* transgenes is described in Chapter 2. *rasa1*$^{fl/fl}$ and *rasa1*$^{fl/fl}$ *pLCK-Cre* HY

TCR Tg and AND TCR Tg mice were generated by cross-breeding with HY TCR Tg or AND TCR Tg mice respectively (purchased from Taconic and JAX respectively). All mice are on a C57BL/6 genetic background. C57BL/6 control mice and B10.BR (H-2^k) mice were purchased from JAX. All mice were 2-3 months of age at the time of experiments. All experiments were performed in compliance with University of Michigan guidelines and were approved by the University Committee on the Use and Care of Animals.

3.13.2 Flow cytometry

Expression of CD4, CD8, CD44, CD25, HY TCR, CD45.1 and CD45.2 upon thymocytes, splenocytes, and LN cells was determined by flow cytometry following cell surface staining with GK1.5-APC-Cy7 (CD4), 53-6.7-PerCP or PE-Cy7 (CD8), IM7-FITC (CD44), PC61-PE (CD25), T3.70-PE (HY TCR), SJL-APC (CD45.1) and 104-PerCP (CD45.2) mAb (BD Biosciences). ERK activation in DP AND TCR Tg thymocytes was determined by additional intracellular staining on cells fixed in ice-cold 90% methanol for 30 minutes using the E10 phospho-ERK specific mAb (Cell Signaling) followed by a PE-coupled rat anti-mouse secondary antibody (BD Biosciences). Cell staining was analyzed on a FACSCanto (BD Biosciences).

3.13.3 Cell isolation

CD4+ and CD8+ T cells were isolated from LN and spleen by negative selection using CD4+ or CD8+ T cell isolation kits (Miltenyi). For the isolation of

CD4+ CD44- T cells from AND TCR Tg mice, a biotinylated CD44 mAb (T2-F4; Abnova) was included in the antibody cocktail mix. Cell populations were greater than 90% pure as determined by flow cytometry. Expression of RASA1 in unfractionated and fractionated cell populations was determined by Western blotting using the B4F8 mAb (Santa Cruz). Blots were stripped and reprobed with either β-actin (C-2) or GAPDH (FL-335) antibodies (both Santa Cruz) to verify equivalent protein loading.

3.13.4 Adoptive transfer experiments

Bone marrow was obtained from C57BL/6 wild type (CD45.1/CD45.2) and *rasa1*$^{fl/fl}$ *Ub-Ert2-Cre* (CD45.2) mice treated with tamoxifen 3 weeks previously (Chapter 2) and was depleted of lineage positive cells by complement-mediated lysis. 5x10^6 wild type and RASA1-defcient bone marrow cells were co-injected into tail veins of lethally-irradiated (950 rad) C57BL/6 wild type recipients (CD45.1). After 6 weeks, recipients were euthanized and thymi were analyzed by flow cytometry. For CD8+ T cell adoptive transfer experiments, CD8+ T cells, purified from the spleens and LN of wild type C57BL/6 and *rasa1*$^{fl/fl}$ *Ub-Ert2-Cre* mice treated with tamoxifen 5 weeks beforehand, were labeled with CFSE (Molecular Probes) and 5x10^6 cells were injected into the tail veins of C57BL/6 wild type recipients. Two weeks later, mice were euthanized and CFSE+ cells in spleen and LN were detected by flow cytometry.

3.13.5 T cell stimulation

$2x10^5$ CD8+ T cells from female HY TCR Tg mice and CD4+CD44- T cells from AND TCR Tg mice were stimulated with $1x10^6$ irradiated splenic adherent cells from female C57BL/6 or B10.BR mice with different concentrations of HY or PCC peptide respectively in complete RPMI medium (10% FBS, 10mM Hepes pH 7.4, Penicillin/Streptomycin, 1mM sodium pyruvate, 50μM β-mercaptoethanol) in wells of 96 well U-bottomed plates. Concentrations of IL-2 and IFN-γ in culture supernatants were determined by ELISA after 48 h (R&D Systems). To examine ERK activation, similar cultures were initiated in microcentrifuge tubes using $1.5x10^6$ each of responder cells and stimulator cells that had been pre-pulsed with peptide (10 μg/ml) for 1 h at 37°C. Cells were co-pelleted and transferred to 37°C for different times before lysis in 1% NP-40 lysis buffer. Activation of ERK was assessed by Western blotting of lysates using the E10 phospho-ERK mAb. Blots were stripped and reprobed with an ERK2 antibody (137F5; Santa Cruz) to ascertain equivalent protein loading.

Chapter 4

Induced systemic deletion of RASA1 from adult mice results in extensive lymphatic hyperplasia and death by chylothorax

4.1 Abstract

RASA1 functions as a negative regulator of the Ras small GTP-binding protein that controls the growth and differentiation of numerous cell types. The importance of RASA1 for normal cell functioning is shown by the finding that non-conditional deletion of RASA1 in mice results in vascular and neuronal developmental defects and embryonic lethality. Furthermore, in humans, germline mutations of the RASA1 gene have been shown to cause a blood vascular disorder known as CM-AVM. To study the role of RASA1 further, we utilized a conditional RASA1-deficient mouse mutant in which expression of RASA1 can be ablated in all tissues in response to drug administration. Deletion of RASA1 in adult mice resulted in a lymphatic vessel leakage defect and death by chylothorax. Moreover, induced RASA1-deficient mice demonstrated a striking extensive systemic lymphatic hyperplasia, although lymph flow rates in collecting lymphatic vessels were normal. Lymphatic disease in induced RASA1-deficient

mice was associated with hyper-activation of the Ras signaling pathway in lymphatic endothelial cells. These findings illustrate an essential role for RASA1 as a regulator of the growth and function of the lymphatic vasculature in mammals.

4.2 Introduction

Ras is an inner membrane-tethered small GTP-binding protein that regulates numerous cell processes including cell growth and differentiation (2). Ras cycles between inactive GDP-bound and active GTP-bound states. Growth factor receptors trigger activation of Ras by recruitment of RasGEFs to membranes which then eject GDP from the Ras guanine nucleotide-binding pocket allowing Ras to bind GTP (11). Activated Ras is recognized by Ras effector molecules which initiate different downstream signal transduction pathways including MAPK pathway (9). Inactivation of Ras is mediated by RasGAPs (11, 12). Upon physical interaction with Ras, RasGAPs accelerate Ras-mediated hydrolysis of GTP by several orders of magnitude. At least ten different RasGAPs have been identified in humans. Amongst these, RASA1 was one of the first described and has since been implicated as a negative-feedback regulator of the Ras signaling pathway initiated through several different growth factor receptors. These include the platelet-derived growth factor receptor (PDGFR), the epidermal growth factor receptor, and the Ephrin receptor B2 (19, 21, 73). In addition, RASA1 has also been shown to regulate certain cellular responses such as directed migration and cell survival in a manner that is

independent of its ability to inactivate Ras (25, 28). Testimony to the importance of RASA1 as a regulator of cell function, homozygous RASA1-deficient mice die at day 10.5 of embryonic development (32). Death is associated with defective development of the blood vascular system and increased neuronal apoptosis.

Recently, a novel clinical disorder known as CM-AVM has been shown to be caused by germline mutations of RASA1 (33-36). CM-AVM is characterized by the presence of randomly-distributed single or multiple pink cutaneous lesions, the underlying cause of which is capillary malformation. In addition, in about one-third of patients, there are fast flow lesions including intracranial arteriovenous malformations, arteriovenous fistulas and Parkes-Weber Syndrome. Ninety-six percent of individuals with RASA1 mutations in thirty-five affected families present with CM-AVM, thus attesting to the penetrance of the phenotype. Mutations in CM-AVM patients are distributed randomly throughout the RASA1 gene and include nonsense, missense and splice-site substitutions as well as insertions and deletions resulting in frame shifts or splice-site disruption. Only one germline RASA1 allele is affected and it is hypothesized that disease results from somatic mutation of the unaffected allele, consistent with the focal nature of lesions.

To further study the importance of RASA1 for the normal functioning of different cell types in adults, we recently generated a conditional floxed allele of *rasa1* in mice (Chapter 2). In this mouse, Cre-mediated recombination results in ablation of RASA1 expression in targeted tissues. In one Cre Tg line that we have utilized, Cre is expressed ubiquitously but is only able to recombine DNA

upon administration to mice of the drug tamoxifen. Therefore, we have used this line to study the effect of RASA1 inactivation in all tissues of adults. We report that systemic deletion of RASA1 from adults does not lead to blood vascular defects. Instead, mice develop a disorder of the lymphatic vascular system.

The lymphatic network of higher eukaryotes is a unidirectional transport system essential for the return of extravasated interstitial fluid or lymph from the tissues to blood, for the absorption of intestinal lipids, and for the efficient trafficking of antigens and immune cells (94, 95). Lymph fluid and antigen-bearing dendritic cells are collected from tissues by open-ended lymphatic capillaries that can be found in the great majority of blood-vascularized sites. From the lymphatic capillaries, fluid and cells then pass into lymphatic collecting vessels which, as afferent lymphatics, transport their contents into lymph nodes. Within lymph nodes, antigen-specific T and B lymphocytes discriminate between antigens that are harmless and those that are a threat to the host and respond accordingly. Lymph that contains recirculating quiescent lymphocytes and/or recently activated lymphocytes exits lymph nodes through efferent collecting lymphatic vessels that eventually drain into the thoracic or right lymphatic ducts. The contents of these ducts are then emptied into the jugular and subclavian veins and thus re-enter the blood circulatory system. Lymph rich in lipid in the form of chylomicrons is also collected from the gut into a specialized sac known as the cisternae chyli, which is continuous with the thoracic duct. Through this route, therefore, intestinal lipids can enter the blood circulation.

Lymphatic capillaries are simple structures made up of a single layer of overlapping endothelial cells with an absence of tight or adherens junctions. Unlike capillaries of the blood vascular system, lymphatic capillaries essentially lack basement membrane and smooth muscle coverage. This permits ready passage of tissue interstitial fluid and immunocytes into the lumen of the capillary. Because they lack smooth muscle cell coverage, lymphatic capillaries have no intrinsic contractile activity. Instead, the propulsive force for lymph flow to collecting vessels is provided by incidental contractions of skeletal muscles. In contrast to lymphatic capillaries, lymphatic collecting vessels have complete basement membrane coverage and are associated with smooth muscle cells, and thus have intrinsic contractile activity which propels lymph toward the central lymphatics. Lymph flow in collecting lymphatics is facilitated by a system of valves that prevent retrograde flow of lymph back to capillaries.

After years of controversy, the mammalian lymphatic system is now known to be exclusively of venous origin (94-97). In mid-gestation (E10-E11 in mice), endothelial cells from the anterior cardinal vein sprout and form primary lymph sacs. The peripheral lymphatic vasculature is then formed by sprouting from several different lymph sacs (E11.5-E14), followed by merging of different capillary networks and remodeling to establish the mature lymphatic capillary network (E14.5-postnatal). In adults, endothelial cells of the lymphatic vasculature are considered quiescent. However, lymphangiogenesis (the sprouting of new lymphatic vessels from existing vessels) occurs readily in response to inflammation, tumor growth, tissue regeneration and wound healing.

In comparison with the blood vascular system, relatively little is known of the molecular mechanisms that regulate the development and function of the lymphatic system. A significant advance in molecular lymphology was the discovery of a transcription factor, Prox-1, that specifies lymphatic endothelial cell (LEC) fate (98, 99). Prox-1 is first expressed in anterior cardinal vein endothelial cells at E9.5. At this point in development, the Prox-1+ endothelial cells also express lymphatic endothelial hyaluronan receptor-1 (LYVE-1) and a receptor tyrosine kinase (RTK) known as vascular endothelial growth factor receptor-3 (VEGFR3), both of which are relatively restricted in expression to LECs (100, 101). Primary lymph sac development is initiated upon interaction of VEGFR3 with its ligand, VEGF-C, on Prox-1+ endothelial cells (102). In addition, VEGF-C interaction with VEGFR3 promotes continued development of the lymphatic system until 2 weeks after birth (103, 104). Accordingly, gene-targeted mice that lack Prox-1 or VEGF-C show severe defects in lymphatic development. In Prox-1-deficient mice, primary lymph sacs form, but endothelial cells within these sacs fail to adopt a lymphatic phenotype. In contrast, in VEGF-C-deficient mice, initial sprouting and directed migration of LECs from veins is blocked. As further evidence for the important role of VEGF-C interaction with VEGFR3, missense mutations of VEGFR3 have been described that result in lymphatic hypoplasia and lymphedema in both mice and humans (105-107).

Apart from VEGF-C, other RTK-RTK ligand systems that have been implicated in lymphatic development include the Tie2 receptor-Angiopoeitin-1/2 (Ang-1/2), platelet-derived growth factor receptor (PDGFR)-PDGF and Ephrin

HB4 receptor-Ephrin B2 systems. Gene-targeted mice that lack Ang-2 show a hypoplastic lymphatic capillary network and disorganized collecting lymphatics with poorly-associated smooth muscle cells (108). These defects can be rescued by Ang-1 which, like VEGF-C and PDGF, shows potent lymphangiogenic activity in adult mice *in vivo* (108-114). Mice that express a form of Ephrin-B2 that lacks binding sites for PDZ-domain-containing proteins in its cytoplasmic domain show several lymphatic abnormalities including hypoplastic collecting lymphatics with defective valves and abnormal sprouting of LECs (115). At 3 weeks of age, the Ephrin B2 mutant mice develop chylothorax, which causes lung compression and death through suffocation. Chylothorax and/or chylous ascites have also been reported in other gene-targeted mouse models, thus pointing to the function of the targeted gene in the regulation of lymphatic function. These include mice that lack expression of the alpha-9 integrin, the Net ternary complex transcription factor and the lipid kinase PI3K (116-119).

4.3 Induced loss of RASA1 expression from adult mice results in death by chylothorax

Mice that carry conditional floxed rasa1 alleles and Ub-Ert2-Cre are described in Chapter 2. To examine the role played by RASA1 in adult tissues, groups of *rasa1*$^{fl/fl}$ *Ub-Ert2-Cre* and control *rasa1*$^{fl/fl}$ mice were given two intraperitoneal injections of tamoxifen at 2 months of age. Despite that in *rasa1*$^{fl/fl}$ *Ub-Ert2-Cre* mice this treatment regimen results in loss of RASA1 expression in

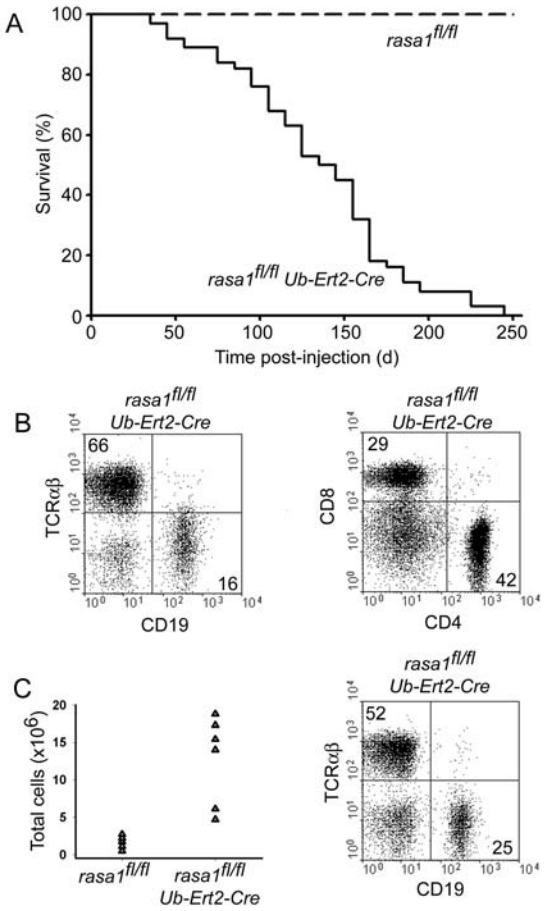

Figure 15: Induced loss of RASA1 expression in adult mice results in early mortality associated with chylothorax and chylous ascites. (A) Kaplan-Meier survival plots of *rasa1*$^{fl/fl}$ *Ub-Ert2-Cre* Tg and *rasa1*$^{fl/fl}$ control mice treated with tamoxifen at 2 months of age (n=50 of each genotype). **(B)** Flow cytometric analysis of pleural effusion cells from deceased tamoxifen-treated *rasa1*$^{fl/fl}$ *Ub-Ert2-Cre* Tg mice showing expression of the indicated lymphocytic markers. **(C)** Total numbers and flow cytometric analysis of peritoneal leukocytes obtained by lavage of *rasa1*$^{fl/fl}$ *Ub-Ert2-Cre* Tg and *rasa1*$^{fl/fl}$ control mice treated with tamoxifen 3 months previously. In B and C, numbers in flow cytometry plots indicate percentage of live cells.

all tissues within 1 week, mice remained healthy for up to 6 weeks after tamoxifen administration (Figure 15A). However, after this time, *rasa1*$^{fl/fl}$ *Ub-Ert2-Cre* mice began to die. Fifty percent were dead at 5 months and all were dead by 8 months post-tamoxifen administration. No deaths were observed in the control group during this time. Prior to death, mice frequently showed signs of labored

breathing, and upon necropsy the thoracic cavity was seen to be filled with a milky-white fluid. Centrifugation of the pleural effusion revealed a cell pellet, an aqueous layer and an apparent upper lipid layer. Biochemical analysis confirmed the high content of triglycerides in the effusion that ranged from 240 to 1200 mg/dL (n=7) which is much higher than that observed in serum. Flow cytometric analysis of the fluid showed that the majority of cells were lymphocytes (>80%). Monocytes and granulocytes were minority populations (Figure 15B). Thus, the fluid has all of the characteristics of chyle (lipid-laden lymph), the accumulation of which in the thoracic cavity presumably suffocates mice leading to death by chylothorax (120).

4.4 Induced RASA1-deficient mice show a generalized lymphatic leakage defect

Leakage of lymph was not confined to the thoracic space since a number of deceased mice also showed visible signs of chylous ascites (effusion of chyle in to the peritoneal cavity). Furthermore, flow cytometric analysis of peritoneal lavages of groups of mice, treated with tamoxifen 3 months previously, consistently revealed the presence of large numbers of leukocytes, the majority of which were again lymphocytes (Figure 15C). These findings suggested that loss of RASA1 expression in adult mice results in a general lymphatic leakage defect. To confirm this, we performed Evans Blue tracing studies. Mice treated with tamoxifen 3 months previously were injected with Evans Blue in the hind footpads and base of the tail. After 1 h, mice were euthanized and drainage of

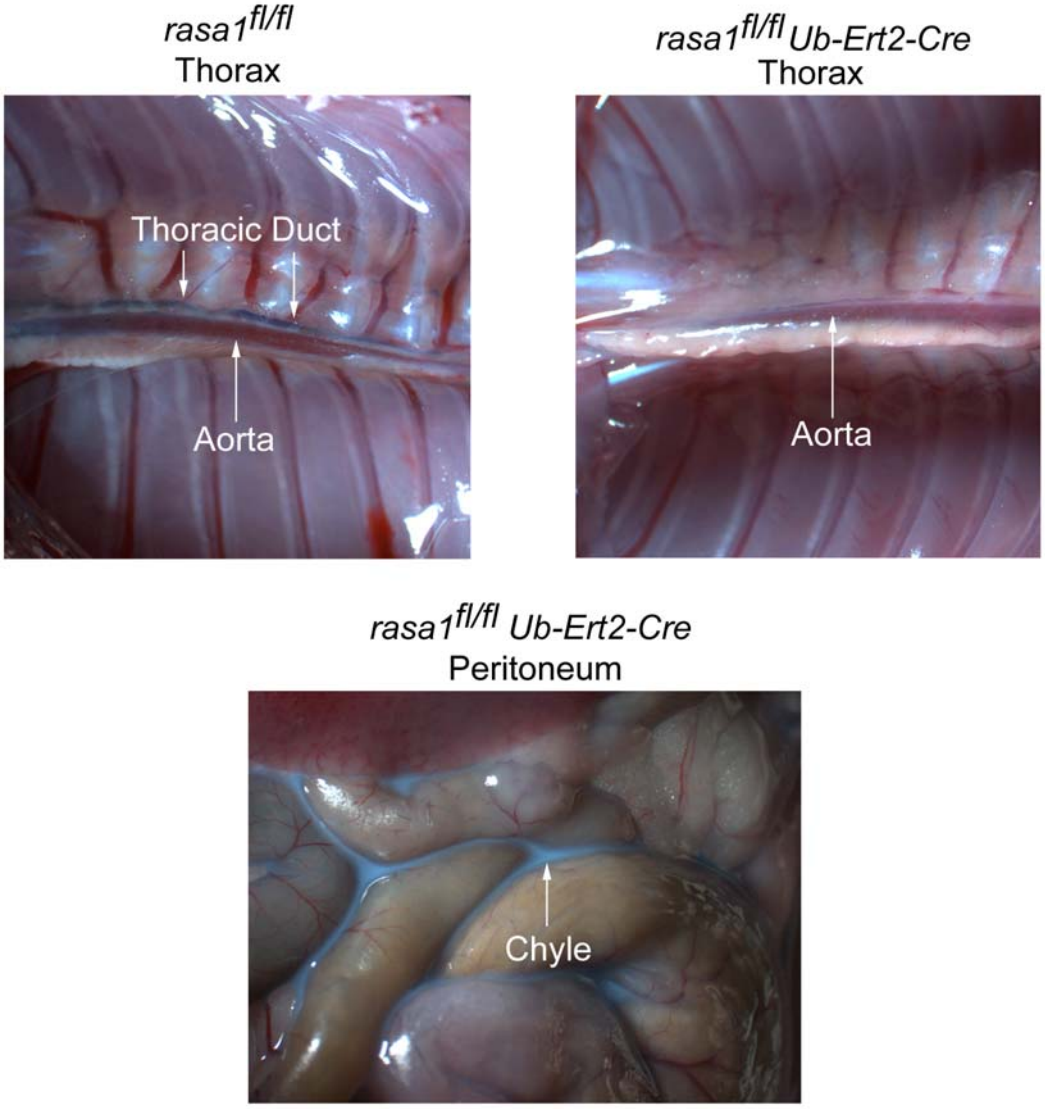

Figure 16: Lymphatic vessel leakage in induced RASA1-deficient mice. Evans Blue dye was injected subcutaneously into the hind footpads and base of the tail *of rasa1$^{fl/fl}$ Ub-Ert2-Cre* and *rasa1$^{fl/fl}$* mice treated with tamoxifen 3 months previously. Drainage of dye into the thoracic duct was examined 1h after injection. A blue thoracic duct is clearly visible in *rasa1$^{fl/fl}$* but not in *rasa1$^{fl/fl}$ Ub-Ert2-Cre* mice. Instead, in *rasa1$^{fl/fl}$ Ub-Ert2-Cre* mice, injected dye commonly drains into the peritoneum.

dye into the thoracic duct was examined (Figure 16). In tamoxifen-treated

rasa1$^{fl/fl}$ mice, dye was readily detected in the thoracic duct to which it gains

access via the cisternae chyli. In contrast, in tamoxifen-treated *rasa1*$^{fl/fl}$ *Ub-Ert2-Cre* mice, drainage of dye to the thoracic duct was never observed. Instead, dye often leaked into the peritoneal cavity of mice presenting as blue chyle (Figure 16).

4.5 Lymphatic vessel distension and hyperplasia in the chest wall of RASA1-deficient mice

Chylothorax that occurs perinatally has been reported in some other mutant mouse models (115-117). In these models, chylothorax is often associated with dilation of thoracic lymphatic vessels. Therefore, to examine if thoracic lymphatics of induced RASA1-deficient mice also show evidence of dilation, we performed immunohistochemical studies of the chest region using an antibody against LYVE-1, a lymphatic endothelium-specific hyaluronan receptor (Figure 17A). As shown, lymphatic vessels of the chest wall were indeed dilated in *rasa1*$^{fl/fl}$ *Ub-Ert2-Cre* mice treated with tamoxifen several months beforehand. However, more striking than this was a large increase in the number of thoracic lymphatic vessels in these mice. This was observed both within the chest wall and on the inside of the chest wall facing the pleural cavity. In fact, in control mice, lymphatic vessels were difficult to identify in the latter location. By contrast, in *rasa1*$^{fl/fl}$ *Ub-Ert2-Cre* mice, there was almost continuous coverage of the pleural face of the chest wall with lymphatics (Figure 17B). As revealed by

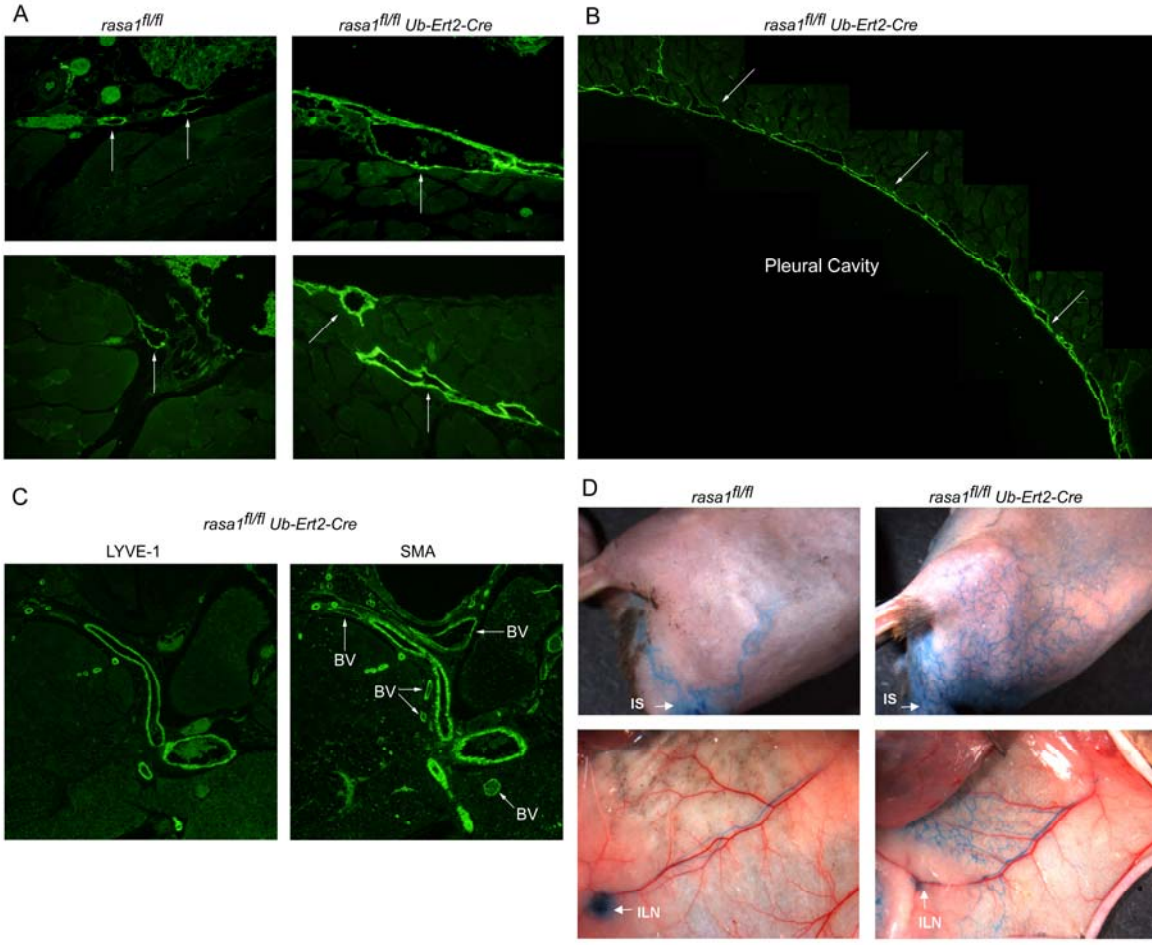

Figure 17: Lymphatic vessel distension and hyperplasia in induced RASA1-deficient mice. (A) Thorax sections of *rasa1*$^{fl/fl}$ *Ub-Ert2-Cre* and *rasa1*$^{fl/fl}$ mice treated with tamoxifen 4 months previously were stained with an anti-LYVE-1 antibody to identify lymphatic vessels. Shown are representative lymphatic vessels (arrows) within the chest wall of both types of mice (X 400). Note the dilation of lymphatics in the *rasa1*$^{fl/fl}$ *Ub-Ert2-Cre* mice **(B)** Shown is a composite of lower power images (X 40) of the chest wall of *rasa1*$^{fl/fl}$ *Ub-Ert2-Cre* mice stained with anti-LYVE-1. The entire of the chest wall facing the pleural space shows lymphatic vessel coverage. By contrast, lymphatic vessels are difficult to identify in this location in control mice (not shown). **(C)** Serial sections of the chest wall of tamoxifen-treated *rasa1*$^{fl/fl}$ *Ub-Ert2-Cre* mice were stained with anti-LYVE-1 or anti-smooth muscle actin (SMA) antibodies. Note that not all LYVE-1 positive vessels have smooth muscle cell coverage. Note also blood vessels (BV), some of which are indicated (X 100). **(D)** Evans Blue was injected intradermally at the base of the tail of shaved *rasa1*$^{fl/fl}$ *Ub-Ert2-Cre* and *rasa1*$^{fl/fl}$ mice treated with tamoxifen 4 months previously. The dermal lymphatic network draining the injection site (IS) was imaged after 1 minute (top). After 4 minutes, a midline incision was made to expose lymphatic vessels and the inguinal LN (ILN) on the underside of the skin (bottom). Note the diffuse dermal lymphatic network in *rasa1*$^{fl/fl}$ *Ub-Ert2-Cre* mice.

staining of serial sections of the chest wall with an antibody against smooth muscle actin, the majority of the thoracic lymphatics in *rasa1*$^{fl/fl}$ *Ub-Ert2-Cre* mice were found to be intimately associated with smooth muscle cells (Figure 17C). This could point to their identity as collecting lymphatic vessels that are distinguished from lymphatic capillaries by smooth cell coverage (94). Alternatively, as reported in some other models of lymphatic dysfunction, there may be abnormal coverage of lymphatic capillaries with smooth muscle cells, at least in the thoracic region, in induced RASA1-deficient mice (121).

4.6 Hyperplasia of dermal lymphatic vessels in induced RASA1-deficient mice

Lymphatic hyperplasia was also noted in other locations such as heart and skin. In skin, this was readily apparent after intradermal injection of shaved mice with Evans Blue at the base of the tail (Figure 17D). In control mice, 1 min after injection, dye was detected in a small number of lymphatics draining toward the inguinal lymph node (LN). However, in *rasa1*$^{fl/fl}$ *Ub-Ert2-Cre* mice at the same time point, dye was identified within a diffuse lymphatic network that radiated from the site of injection, although dye eventually reached the inguinal LN, as in controls.

4.7 Lack of blood vascular lesions in induced RASA1-deficient mice

Because RASA1 mutations cause CM-AVM in humans, we looked carefully for blood vascular abnormalities in induced RASA1-deficient

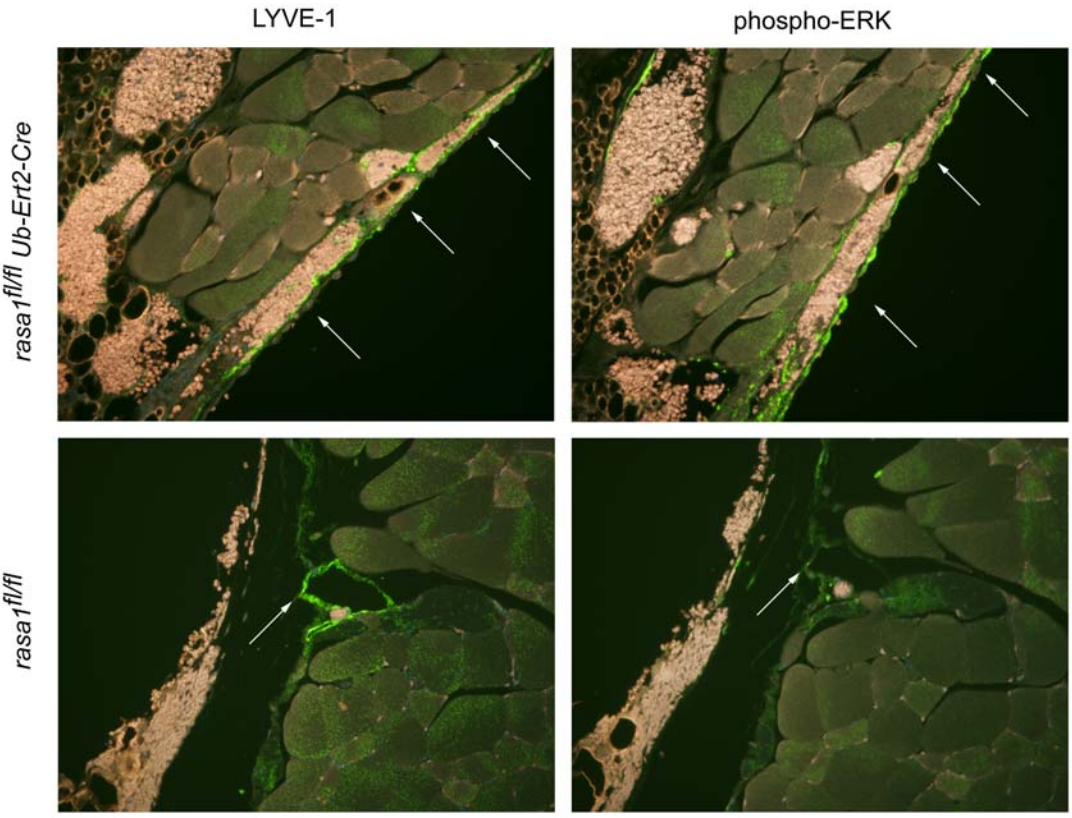

Figure 18: Constitutive activation of ERK MAPK in thoracic lymphatics of induced RASA1-deficient mice. Serial sections of the chest wall of *rasa1*$^{fl/fl}$ *Ub-Ert2-Cre* and *rasa1*$^{fl/fl}$ mice treated with tamoxifen 4 months previously were stained with an antibody against the lymphatic endothelial cell-specific hyaluronan receptor LYVE-1 (left) or an anti-phospho ERK antibody (right) (X 400). Images were acquired using a pan-RGB fluorescence filter. Note the constitutive activation of ERKs (green) in lymphatics of *rasa1*$^{fl/fl}$ *Ub-Ert2-Cre* mice but not *rasa1*$^{fl/fl}$ mice. Note also the presence of erythrocytes (red autofluorescence) in the lymphatic vessels of the *rasa1*$^{fl/fl}$ *Ub-Ert2-Cre* mouse. The presence of erythrocytes in lymphatic vessels has been observed in other models of chylothorax.

mice. There was no evidence of any capillary malformations in any tissue. Likewise, there was no evidence of fast flow lesions including arteriovenous malformations (intracranially or otherwise) or arteriovenous fistulas and no evidence of lesions resembling Parkes Weber syndrome (data not shown). Thus,

as far as we can determine, vascular lesions in induced RASA1-deficient mice are specific to the lymphatic system.

4.8 Constitutive activation of ERK MAPK in lymphatic endothelium of induced RASA1-deficient mice

Since RASA1 functions as a negative regulator of Ras signal transduction, we next asked if there was any evidence of increased activation of Ras in lymphatic endothelium of induced RASA1-deficient mice. For this purpose, we examined the activation of MAPK by immunohistochemistry using phospho-MAPK antibodies (Figure 18). Lymphatic vessels within the chest walls of tamoxifen-treated *rasa1*$^{fl/fl}$ *Ub-Ert2-Cre* mice showed constitutive activation of MAPK, in contrast to lymphatic vessels within the chest walls of tamoxifen-treated control mice which did not. Interestingly, blood vessel endothelium of tamoxifen-treated *rasa1*$^{fl/fl}$ *Ub-Ert2-Cre* mice also frequently showed constitutive MAPK activation despite that there were no abnormalities of blood vessel structure (Figure 18).

4.9 Lymph flow rates in lymphatic vessels of induced RASA1-deficient mice

To study the lymphatic defect in induced RASA1-deficient mice further, we performed dynamic non-invasive near infrared imaging studies of lymph flow in live mice (122). For this purpose, tamoxifen-treated *rasa1*$^{fl/fl}$ *Ub-Ert2-Cre* and *rasa1*$^{fl/fl}$ mice were injected with indocyanine green (IC-Green) intradermally at the base of the tail. Fluorescence images were then acquired for up to 20 min

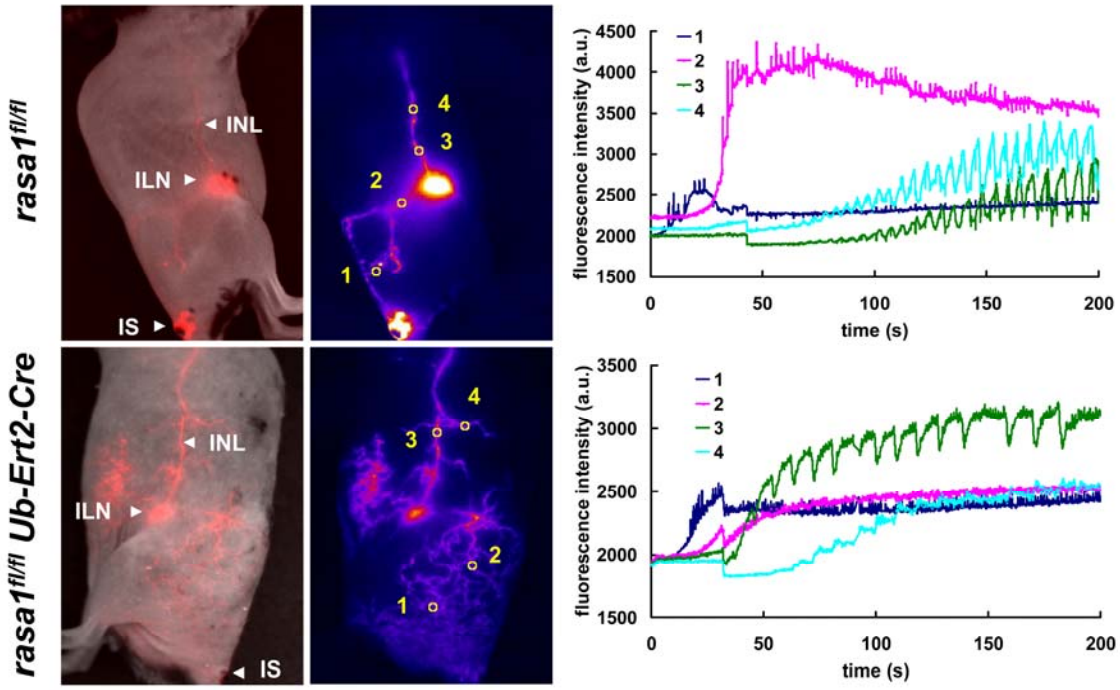

Figure 19: Quantitative analysis of lymph flow in induced RASA1-deficient mice. *rasa1*$^{fl/fl}$ *Ub-Ert2-Cre* and *rasa1*$^{fl/fl}$ mice treated with tamoxifen 4 months previously were injected intradermally at the base of the tail with IC-Green. At left are shown fluorescence images of live animals (one with a superimposed light image and one without) acquired at a 3 min timepoint after injection. INL, inguinal to axillary internodal lymphatic vessel. Numbered select regions of interest (ROI) within the lymphatic network are shown. Plots at right depict fluorescence intensity for each ROI with respect to time after injection. Features to note include the absence of contractile activity in lymphatic vessels draining the site of injection in each mouse, a similar frequency of contractile activity in collecting lymphatics of mice, and a lack of contractile activity in lymphatic vessels that branch from the internodal lymphatic vessel in *rasa1*$^{fl/fl}$ *Ub-Ert2-Cre* mice.

(Figure 19). These analyses provided non-invasive confirmation of the extensive lymphatic hyperplasia in induced RASA1-deficient mice. In control mice, dye followed an almost direct route of drainage from the site of injection to the inguinal LN and, subsequently, the axillary LN via an internodal lymphatic vessel. However, in induced RASA1-deficient mice, dye first entered into an expansive

lymphatic vessel network before drainage to inguinal and axillary LN. Another striking feature of the induced RASA1-deficient mice was that numerous lymphatic vessels were seen to branch off from the inguinal to axillary internodal lymphatic vessel. Lymphatic vessel sprouting from this lymphatic channel has not been observed in control mice (Figure 19). For several selected regions of interest (ROI) within the lymphatic network, we analyzed fluorescence intensity with respect to time (Figure 19). These studies revealed an absence of pulsatile activity in the hyperplastic draining lymphatics proximal to the site of injection in induced RASA1-deficient mice. This is consistent with their identity as lymphatic capillaries or newly-formed collecting vessels that have not yet acquired smooth muscle cell coverage (94). Likewise, there was an absence of pulsatile activity in lymphatic vessels that branch from the inguinal to axillary internodal lymphatic in induced RASA1-deficient mice. Pulsatile activity was detected in larger collecting lymphatic vessels of induced RASA1-deficient mice. However, flow rates in these larger vessels were on average not different from that observed in control mice. Thus, lymphatic dysfunction does not appear to result from a loss of an intrinsic inability of vessels to propel lymph. This is in agreement with the absence of any evidence of tissue lymphedema in this model.

4.10 Enhanced growth factor receptor signaling in RASA1-deficient lymphatic endothelial cells

We reasoned that the most likely cause of lymphatic hyperplasia in *rasa1*$^{fl/fl}$ *Ub-Ert2-Cre* mice treated with tamoxifen was abnormal signaling through

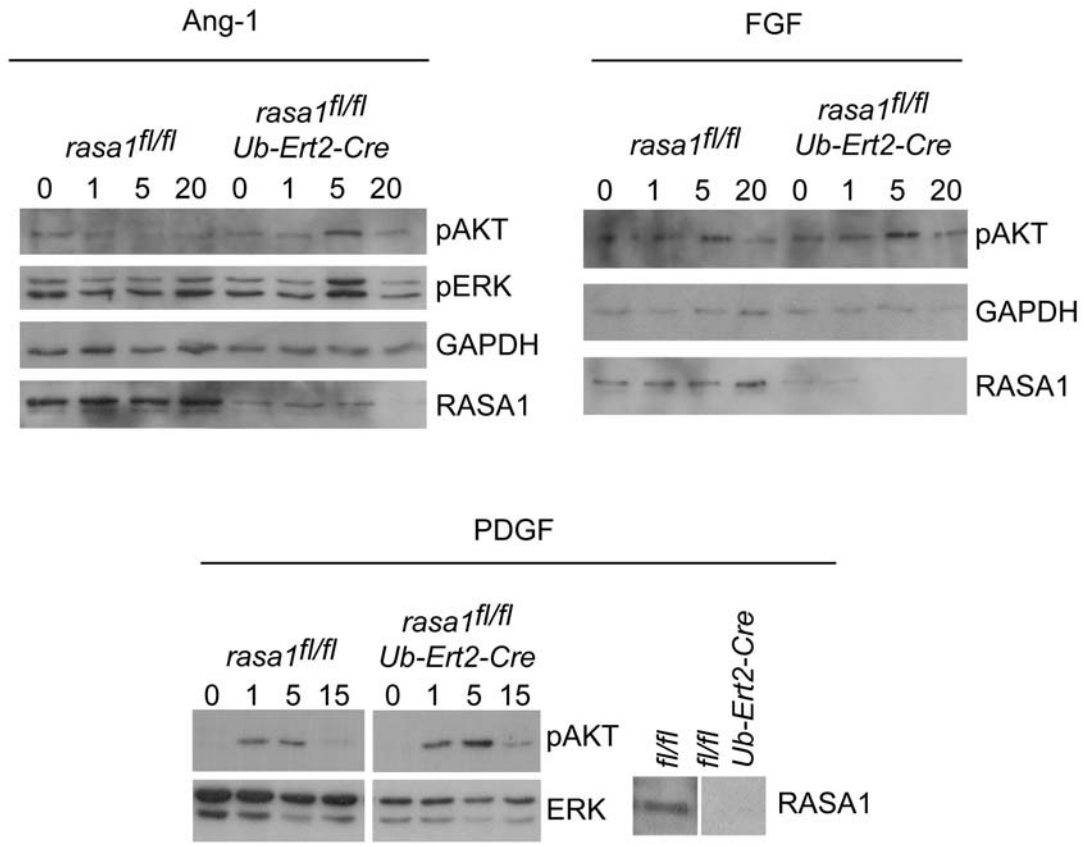

Figure 20: Enhanced growth factor receptor signaling in RASA1-deficient lymphatic endothelial cells. LECs were purified from *rasa1*$^{fl/fl}$ or *rasa1*$^{fl/fl}$ *Ub-Ert2-Cre* mice treated with tamoxifen 5 weeks previously, and treated with 20ng/ml Ang-1, FGF, or PDGF for the indicated times (in minutes). Cells were lysed in NP-40 lysis buffer, and activation of AKT and ERK was determined by Western blotting of lysates using phospho-specific AKT and ERK antibodies, respectively. For each growth factor tested, we observed increased AKT phosphorylation at 5 minutes for RASA1-deficient LECs. In addition, for Ang-1 stimulation we observed increased activation of ERK. These results suggest that RASA1 plays a regulatory role in signaling through multiple growth factor receptors.

a growth factor receptor in LECs. In order to determine the growth factor receptor or receptors responsible, we isolated LECs from *rasa1*$^{fl/fl}$ or *rasa1*$^{fl/fl}$ *Ub-Ert2-Cre* mice treated with tamoxifen 5 weeks previously. Isolated LECs were stained with antibodies against LYVE-1 or VEGFR-3 and analyzed by flow

cytometry to confirm that the cells expressed these LEC-specific markers (not shown). After incubating the cells overnight in serum-free medium, they were stimulated for various times with PDGF, Ang-1, or fibroblast growth factor (FGF), which have each been implicated in the growth of lymphatic vessels. We found that for PDGF, FGF, and Ang-1 stimulation, *rasa1*$^{fl/fl}$ *Ub-Ert2-Cre* LECs had an enhanced activation of AKT compared to *rasa1*$^{fl/fl}$ controls (Figure 20). In addition, there was increased activation of ERK following Ang-1 stimulation in RASA1-deficient LECs. These results suggest that, at least *in vitro*, RASA1 plays a role in regulating signal transduction in LECs from multiple different growth factor receptors, and for at least two distinct signaling cascades.

4.11 Discussion

We show here that induced systemic deletion of RASA1 from adult mice causes a generalized lymphatic leakage defect resulting in chylous ascites, chylothorax and death. Moreover, lymphatic dysfunction in induced RASA1-deficient mice is associated with a profound lymphatic vessel hyperplasia that distinguishes this model from other murine models of chylothorax/chylous ascites or lymphatic dysfunction (94, 95). The precise mechanism by which RASA1 controls lymphatic growth and function in adult animals is unknown. However, based on the above data, it is reasonable to assume that RASA1 normally acts as a negative-regulator of signal transduction through multiple lymphatic endothelium growth factor receptors, including PDGFR, Tie2, and FGFR (Figure 20). Expression of RASA1 might thus be necessary in order to maintain lymphatics in a quiescent state. It is also possible that the increased activation of

AKT leads to enhanced survival of RASA1-deficient LECs, rather than dysregulated proliferation. Another strong candidate receptor that might be dysregulated is the vascular endothelial growth factor receptor-3 (VEGFR3) (94). VEGF-C, in addition to Ang-1 and PDGF, has been shown to function as a potent lymphangiogenic factor *in vivo* (109-113). Furthermore, VEGFR3, Tie2, and PDGFR contain cytoplasmic domain tyrosine residues in canonical motifs that would allow recognition by RASA1 SH2 domains and thus recruitment of RASA1 to membranes during the course of receptor signaling. Indeed, VEGFR3 has been shown to trigger activation of the Ras/MAPK pathway and AKT in LECs *in vitro*. Furthermore, this activation has been shown to be essential for growth and survival of activated LECs (103, 123). Further experiments using adeno-associated virus expressing fusion proteins of ectodomains of various growth factor receptors to inhibit specific growth factor signaling will allow us to determine the importance of RASA1 in each growth factor receptor signaling pathway *in vivo*.

Dysregulated signal transduction through one or more LEC growth factor receptors leading to hyper-activation of the Ras/MAPK pathway would be consistent with our observation that ERKs are constitutively active in LECs of induced RASA1-deficient mice. It has been shown previously that dysregulated Ras/MAPK signaling can cause lymphatic disease in mice, as is the case with mice deficient in the proteins Spred-1 and Spred-2. These proteins are structurally similar to the Sprouty proteins in *Drosophila*, and have been found to be negative regulators of Ras/MAPK signaling (124). Rather than directly

catalyze GTPase activity in Ras, the Spreds inhibit the activation of Raf-1, a downstream mediator of Ras activation. Mice deficient in both Spred-1 and Spred-2 proteins die at embryonic day E12.5 to E15.5 displaying subcutaneous hemorrhage, edema, and dilated lymphatic vessels filled with erythrocytes (125). Further investigation found that the number of LYVE-1 positive LECs was markedly increased in these mice, while the number of blood endothelial cells remained constant. Spreds were found to inhibit signaling through VEGFR3, suggesting that VEGFR3-mediated Ras/MAPK signaling can directly affect lymphatic cell growth. However, it is uncertain if augmented signaling through the Ras pathway, translated through ERK or AKT, is sufficient for the full development of lymphatic disease. In this regard, RASA1 has been shown to regulate certain cellular functions independent of its GAP domain (25, 28). Indeed, it is possible that some aspects of the lymphatic disorder described herein, e.g. hyperplasia, are consequent to dysregulated activation of Ras whereas other aspects of the disorder, e.g. leakage of lymph, are consequent to the dysregulation of a distinct signaling pathway. Resolution of these questions will come with the generation of mice with BAC Tg mutants of RASA1 that are defective in specific activities.

Since humans with RASA1 mutations develop CM-AVM with high penetrance, we were surprised to find no evidence of blood vascular abnormalities in induced RASA1-deficient mice. This could reflect a genuine difference in a requirement for RASA1 for the maintenance of the blood vasculature in adults between species. Alternatively, differences could relate to

the timing of loss of RASA1 expression. In CM-AVM, it may be necessary to incur proposed secondary hit mutations during embryonic development in order for blood vascular abnormalities to develop. In this regard, in mice, deletion of RASA1 during embryogenesis may also result in the development of blood vascular lesions in adults. Certainly, early in mouse embryogenesis, RASA1 plays an essential role in blood vascular endothelial cells as evidenced by an inability of endothelial cells in non-conditional RASA1-deficient mice to organize into a blood vascular network (32).

Conversely to the blood vascular differences noted above, chylothorax and chylous ascites have been observed in a small number of CM-AVM patients (36). Chylothorax and chylous ascites are rare in humans and thus a lymphatic phenotype resulting from loss of RASA1 expression may be conserved across species. It is possible that a larger number of CM-AVM patients show lymphatic abnormalities such as hyperplasia that may be revealed by non-invasive near infrared imaging (126). Alternatively, an apparent lower incidence of lymphatic abnormalities in CM-AVM could be explained by a requirement for second hit mutations in lymphatic endothelial cells which would result in localized lesions as in the blood vasculature in this disease. This contrasts with the induced RASA1-deficient mouse in which the majority of lymphatic endothelial cells would be expected to lose expression of RASA1.

In summary, we show that RASA1 is an essential negative-regulator of the growth of lymphatic vessels and is required for lymphatic vessel functional integrity in adult mice. These findings have important implications for our

understanding of the molecular mechanisms that control lymphatic vessel growth and function in healthy animals. In addition, findings may provide insight into mechanisms by which the lymphatic system may be manipulated for clinical benefit in different diseases such as lymphedema and in cancer where stimulation or inhibition of lymphangiogenesis would be desirable (95).

4.12 Materials and Methods

4.12.1 Mice

rasa1$^{fl/fl}$ mice with and without *Ub-Ert2-Cre* transgenes were generated as described previously (Chapter 2). All mice are on a mixed 129S6/SvEv X C57BL/6 genetic background. At age 2 mo, mice were given two i.p. injections of tamoxifen (MP biochemicals) on consecutive days (0.2 mg/g body weight dissolved in corn oil for each injection). All experiments performed with mice were in compliance with University of Michigan guidelines and were approved by the University committee on the use and care of animals.

4.12.2 Flow cytometry

Pleural effusion cells from deceased *rasa1*$^{fl/fl}$ *Ub-Ert2-Cre* mice and peritoneal exudate cells (obtained by lavage) from euthanized *rasa1*$^{fl/fl}$ and *rasa1*$^{fl/fl}$ *Ub-Ert2-Cre* mice were stained with fluorochrome-labeled TCRβ (H57-597), CD19 (1D3), CD4 (GK1.5) and CD8 (53-6.7) mAb (BD Biosciences). Cell staining was analyzed by flow cytometry on a FACSCanto (BD Biosciences).

4.12.3 Evans Blue tracing studies

For thoracic duct drainage experiments, Evans Blue (Sigma; 5 mg/ml in PBS) was injected s.c. into hind foot pads and the base of the tail (50 µl at each injection site). After 1 h mice were euthanized and drainage of dye to the thoracic duct was examined. For examination of dermal lymphatics, Evans Blue was injected intradermally at the base of the tail of shaved mice (20 µL per injection). Dermal lymphatics were imaged 1 min afterwards. Subsequently, mice were euthanized and a midline incision was made to expose lymphatics on the underside of the skin and the inguinal LN.

4.12.4 Immunohistochemistry

Mice were euthanized and thoraxes were fixed in 4% paraformaldehyde, decalcified and embedded in paraffin. Five micrometer sections of the chest wall were stained with anti-LYVE-1 (Upstate Biotechnology), anti-smooth muscle actin (Sigma) or anti-phospho-ERK (Cell Signaling) primary antibodies followed by a biotin-labeled secondary antibody as described previously (126). A TSA kit (Perkin Elmer) was used for signal detection and amplification. Fluorescence was observed on an Olympus IX70 microscope.

4.12.5 Near infrared imaging

Near infrared imaging was performed as described (122). 25µl of IC-Green (555 µM in 0.9% saline) was injected intradermally at the base of the tail of shaved mice. Fluorescence images were acquired with 100 ms integration

time by an electron-multiplying CCD camera (Princeton Instruments). Data was analyzed with Matlab (The Mathworks) and ImageJ (NIH). Pulsatile activity was determined by measuring the mean fluorescence intensity at select ROI with respect to time.

4.12.6 LEC isolation and stimulation

LECs were isolated by removing lungs from mice, rinsing with PBS, and mincing them and digesting in 0.2% Collagenase II for 90 min at 37°C, then homogenizing and passing through a 70-micron cell strainer. Cells were suspended in binding buffer (PBS, 1% FBS, 2mM EDTA) and incubated with 5μg/ml anti-LYVE-1 (ALY7, MBL International) antibody at 4°C for 15 min. After one wash in binding buffer, the cells were incubated with goat anti-rat magnetic beads (Miltenyi) for 15 min at 4°C. Cells were washed once in binding buffer, purified on LS columns (Miltenyi), and plated in collagen-coated 24 well plates in DMEM, 20% FBS, 10mM Hepes, penicillin/streptomycin, 100μg/m heparin, and 30μg/ml endothelial cell growth supplement (ECGS). The cells were fed once after 5 days, and after 10 days, the confluent cells were detatched from the plates with Accutase (Sigma). Approximately $4x10^4$ cells were plated in wells of a collagen-coated 96 well plate in serum-free DMEM overnight, and stimulated with 20ng/ml of PDGF (BioVision), FGF (Genway Biotech), or Angiopoietin-1 (Axxora).

Chapter 5

Conclusions

5.1 Dissertation Summary

Ras signaling has been shown to be of critical importance in T cells. In an attempt to define which RasGAPs function to negatively regulate Ras in T cells, we chose to study RASA1, the prototypical RasGAP. In this work, we seek to address the following questions; first, does RASA1 indeed play an important role in the regulation of Ras signaling in T cells? Second, does RASA1 play an important role in other systems in adult animals that have not previously been described? In order to address these questions, we developed a conditional RASA1-deficient mouse model to overcome the embryonic lethality that is characteristic of the complete RASA1-deficient model (32).

In Chapter 2, the construction of the conditional *rasa1* allele is described. By flanking exon 18 of the *rasa1* gene with loxP sites, we were able to delete RASA1 protein expression specifically in T cells by crossing *rasa1*$^{fl/fl}$ mice with Tg mice expressing the Cre recombinase under the control of the proximal LCK promoter. We also show that the ubiquitously expressed, tamoxifen-inducible Cre recombinase, Ub-Ert2-Cre, is able to splice the *rasa1*$^{fl/fl}$ allele and extinguish expression in a wide variety of tissues in adult mice. With either form of Cre, we

show that there are no low molecular weight truncations of the RASA1 protein, and that the mRNA is most likely degraded by nonsense-mediated RNA decay. This makes our conditional RASA1-deficient mouse model an ideal tool to study the effects of RASA1-deficiency in a range of cell types.

In Chapter 3, we describe the phenotype of *rasa1*$^{fl/fl}$ *pLCK-Cre* mice, in which RASA1 is specifically deleted early in T cell development. We find that T cell development in the thymus is almost normal. However, in AND TCR Tg mice, we find that there is a modest enhancement in positive selection of CD4+ T cells. The enhanced positive selection was associated with increased MAPK signaling in these cells. Both positive and negative selection were found to be unaffected in RASA1-deficient HY TCR Tg T cells. By adoptive transfer of wild type and RASA1-deficient bone marrow into irradiated wild type hosts, we again demonstrated enhanced positive selection of RASA1-deficient thymocytes. We show that in the peripheral lymphoid organs of T cell-specific RASA1-deficient mice there are a reduced number of T cells, which is most apparent in the CD8+ population. Moreover, a larger percentage of peripheral T cells express the memory marker CD44 in mice deficient in RASA1. By purifying naïve RASA1-deficient CD8+ T cells and injecting into wild type hosts, we show that these cells have significantly decreased survival, which is most likely the cause of lymphopenia in RASA1-deficient animals. Finally, we show that naïve RASA1-deficient T cells purified from HY TCR or AND TCR Tg mice secrete larger amounts of cytokines than do wild type controls, and that this is associated with increased MAPK signaling.

In Chapter 4, we describe the surprising phenotype of adult *rasa1*$^{fl/fl}$ *Ub-Ert2-Cre* mice in which RASA1 expression has been extinguished in all tissues by tamoxifen administration. These mice appear healthy until approximately 6 weeks after induction, at which point they begin to die. Half the mice are dead by approximately 150 days post-induction, and all are dead by 250 days post-induction. Necropsy of dead mice reveals the cause of death to be chylothorax, a condition where lipid-laden lymph leaks from lymphatic vessels into the thoracic cavity, causing suffocation due to compression of the lungs. Injection of Evans Blue dye into footpads of *rasa1*$^{fl/fl}$ *Ub-Ert2-Cre* mice treated with tamoxifen weeks previously shows an abnormal network of hyperplastic lymphatic capillaries branching from existing lymphatic ducts, as well as a lack of drainage of lymph to the thoracic duct, likely due to leakage into the peritoneum. By using immunohistochemical staining, we show a vast proliferation of lymphatic vessels lining the face of the pleural cavity, and that many of these have constitutive MAPK activation. We showed using near-infrared imaging that dermal lymphatic hyperplasia was evident in RASA1-deficient mice, and that hyperplastic lymphatic vessels at this site lacked pulsatile activity, suggesting that they are lymphatic capillaries, or lymphatic collecting ducts that lack smooth muscle coverage. Collecting lymphatic ducts in RASA1-deficient mice, however, showed normal pulsatile activity. Interestingly, we found no evidence of blood vascular malformations in *rasa1*$^{fl/fl}$ *Ub-Ert2-Cre* mice treated with tamoxifen, suggesting that RASA1 does not play a role in maintenance of adult blood vessels, at least under these conditions. Preliminary data show that LECs from

induced RASA1-deficient mice are hyperresponsive to the growth factors PDGF, Ang-1, and FGF *in vitro*.

5.2 Future Directions

The finding that RASA1 is a regulator of Ras signaling in T cells is a significant step in answering the question as to how Ras signaling is controlled in this cell type. However, many questions remain to be addressed. For example, since RASA1 has been shown to function in signaling pathways that do not involve Ras, it is unclear at this point if the role of RASA1 in T cell cytokine secretion relates solely to an ability to regulate Ras, or if it may be explained by involvement in these other signaling pathways. In order to address how much of the phenotype seen in *rasa1*$^{fl/fl}$ *pLCK-Cre* HY TCR or AND TCR Tg T cells is due to an increase in Ras/MAPK signaling, we are generating a Tg mouse model in which a form of RASA1 with a catalytically inactive GAP domain is expressed on a bacterial artificial chromosome (BAC). In this mutant, the catalytic Arginine of the GAP domain is mutated to a Glutamine (R780Q), because this mutation has previously been shown to abrogate GAP activity (127, 128). Making a knock-in mutant where the endogenous *rasa1* gene is mutated was one possible way to proceed, but this mouse would have a high likelihood of dying during embryonic development. By expressing the mutant *rasa1* on a BAC, we can leave the endogenous floxed *rasa1* alleles intact to express the wild type RASA1 protein. Crossing these mice to pLCK-Cre Tg, HY TCR or AND TCR Tg mice will result in the loss of expression of the wild type protein in T cells, leaving expression of

only BAC encoded RASA1 R780Q. By comparing peptide/MHC-induced cytokine synthesis and activation of the Ras/MAPK pathway in these RASA1 R780Q reconstituted, RASA1-deficient, HY TCR or AND TCR Tg T cells, we will determine if loss of the GAP domain activity of RASA1 is solely responsible for the increased cytokine secretion seen in *rasa1*$^{fl/fl}$ *pLCK-Cre* mice. We predict that the RASA1 R780Q reconstituted, RASA1-deficient T cells will secrete greater quantities of cytokines and show increased RAS/MAPK signaling upon stimulation with MHC-peptide, similar to the RASA1-deficient cells discussed above.

If by using the GAP-domain mutant RASA1 BAC Tg model we discover that the GAP domain is solely responsible for the T cell phenotype, we will also be able to ask which of the other modular binding domains of RASA1 are required for the negative-regulation of T cell cytokine synthesis by generating *rasa1* BACs in which the modular binding domains have been mutated. Since the SH2 domains of RASA1 have been implicated in RASA1 targeting to Ras in fibroblasts, and the PH domain has a known role in targeting of proteins to lipids, these will be our first targets of inactivating mutations (19-22, 129). In RASA1-deficient T cells reconstituted with mutant RASA1 BACs, we would expect that cytokine secretion would be increased and RAS/MAPK activation would be enhanced compared to T cells containing wild type RASA1 BACs. The results should point to a role of the individual domains in the targeting of RASA1 to Ras during the process of TCR signal transduction.

The development of lymphatic disease in *rasa1*$^{fl/fl}$ *Ub-Ert2-Cre* mice treated with tamoxifen is a striking result. However, as the Cre recombinase is expressed in all tissues as a result of the ubiquitin promoter, it is not possible to determine if the lymphatic hyperplasia seen in these mice is solely due to lymphatic endothelial cell dysfunction. As shown in Chapter 4, a prediction of the dysregulated growth factor signaling hypothesis in LECs is that the lymphatic defect is intrinsic to LECs (Figure 20). To test this hypothesis, we have obtained Tg mice that express Ert2-Cre under the control of the LEC-specific transcription factor promoter, Prox-1 (96, 130). This Prox1-Ert2-Cre strain has been shown to be useful for the deletion of floxed genes in a relatively LEC-restricted manner. These mice will be crossed with *rasa1*$^{fl/fl}$ mice and tamoxifen will be administered to the resulting *rasa1*$^{fl/fl}$ *Prox1-Ert2-Cre* progeny. The development of chylothorax and chylous ascites in the animals will then be monitored. Tissue sections of the chest wall as well as skin will be stained by immunohistochemistry with LYVE-1 antibodies to evaluate the extent of lymphatic hyperplasia. In addition, these mice will be subject to analysis of lymph flow by near-infrared imaging. We predict that *rasa1*$^{fl/fl}$ *Prox1-Ert2-Cre* mice will show the same mortality and lymphatic abnormalities as *rasa1*$^{fl/fl}$ *Ub-Ert2-Cre* mice, suggesting that lymphatic disease is directly attributable to the absence of RASA1 in LECs.

The RASA1-mutant BAC transgene system described above for the proposed T cell experiments will also be useful in studying the lymphatic disease in *rasa1*$^{fl/fl}$ *Ub-Ert2-Cre* mice. Injecting the wild type or mutant *rasa1* BACs into fertilized embryos of *rasa1*$^{fl/fl}$ *Ub-Ert2-Cre* mice will produce animals that express

the mutant form of *rasa1* in addition to the wild type proteins. Administration of tamoxifen will extinguish expression of wild type RASA1, leaving only the mutant form to be expressed. By studying the survival of *rasa1*$^{fl/fl}$ *Ub-Ert2-Cre* mice that have either wild type or GAP-mutant forms of the *rasa1* BAC, we will be able to determine which specific domains of RASA1 are responsible for the maintenance of lymphatic vessels. We predict, although are not certain, that mice expressing the GAP-mutant form of RASA1 will display lymphatic hyperplasia to the same extent as *rasa1*$^{fl/fl}$ *Ub-Ert2-Cre* mice that have been treated with tamoxifen. This would demonstrate that Ras hyper-activity is sufficient to induce the lymphatic disease that results from the loss of expression of RASA1. However, it is also possible that these mice will only display a partial disease phenotype, since the interaction of RASA1 R780Q with AKT and p190 RhoGAP would be expected to remain intact.

If the Ras hyper-activation is found to be responsible for lymphatic hyperplasia, a next logical step would be to determine if there is a specific extracellular signal that is dysregulated. In chapter 4, the stimulation of LECs *in vitro* with growth factors is discussed, and *rasa1*$^{fl/fl}$ *Ub-Ert2-Cre* LECs were found to have abnormal AKT activation in response to PDGF, Ang-1, and FGF. In addition, enhanced Ras/MAPK signaling was observed when stimulated with Ang-1. However, culturing LECs is time consuming, and the number of cells recovered is low, limiting the number of experiments that can be performed. Since it is unknown how extended *in vitro* culture affects LECs, it is important to study which growth factor receptor is dysregulated *in vivo*. In order to answer the

question of which growth factor receptor is dysregulated in *rasa1*$^{fl/fl}$ *Ub-Ert2-Cre* mice *in vivo*, we will perform Matrigel (BD Biosciences) plug assays. This assay involves the subcutaneous injection into mice of Matrigel, a mixture of extracellular matrix proteins that is a liquid at low temperature, and solidifies into a gel plug at body temperature (131, 132). Different growth factors will be added to the Matrigel while in liquid form, and injected subcutaneously into *rasa1*$^{fl/fl}$ or *rasa1*$^{fl/fl}$ *Ub-Ert2-Cre* mice that have previously been treated with tamoxifen. After 10 days, the matrigel plug will be removed, fixed in paraformaldehyde, and mounted in paraffin for immunohistochemistry. By staining with anti-LYVE-1 antibodies, we will be able to assess the extent of lymphatic infiltration into the Matrigel plug, thus providing a way of evaluating the effects of single growth factors on LECs in inducing lymphatic hyperplasia in RASA1-deficent animals *in vivo*.

Perhaps the most definitive way to identify which receptors in LECs are dysregulated is to perform *in vivo* receptor blocking studies. Blockade of the interaction of a dysregulated growth factor receptor with its ligand prior to the induction of RASA1 loss should prevent the subsequent development of lymphatic hyperplasia. This could be achieved by administration to mice of specific antibodies to receptors or ligands, or by administration of purified soluble ectodomains of receptors in the form of immunoglobulin Fc fusion proteins, which act as ligand decoys (104, 133). Both of these approaches have the disadvantage that they require repeated injections of reagents over an extended period of time. Instead, we plan to use an adeno-associated virus gene delivery

approach to express receptor ectodomains systemically and inhibit receptor-ligand interactions *in vivo*. Previous studies have shown the effectiveness of adenoviral-mediated delivery of a VEGFR3-human IgG1 Fc fusion protein as a means of blocking VEGF-C interaction with VEGFR3 in mice (104, 133-135). We will generate viruses expressing ectodomains of growth factor receptors fused to IgG Fc, including VEGFR3, PDGFR, FGFR, and Tie2, as well as control viruses expressing IgG Fc only. By comparing the lymphatic hyperplasia from *rasa1*$^{fl/fl}$ *Ub-Ert2-Cre* mice treated with tamoxifen as well as fusion-protein expressing virus or control virus, we will be able to determine which growth factor receptor is dysregulated in RASA1 deficient LECs.

References

1. Campbell, S. L., R. Khosravi-Far, et al. (1998). "Increasing complexity of Ras signaling." Oncogene **17**(11 Reviews): 1395-413.
2. Wennerberg, K., K. L. Rossman, et al. (2005). "The Ras superfamily at a glance." J Cell Sci **118**(Pt 5): 843-6.
3. Matozaki, T., H. Nakanishi, et al. (2000). "Small G-protein networks: their crosstalk and signal cascades." Cell Signal **12**(8): 515-24.
4. Olson, M. F. and R. Marais (2000). "Ras protein signalling." Semin Immunol **12**(1): 63-73.
5. Reuter, C. W., M. A. Morgan, et al. (2000). "Targeting the Ras signaling pathway: a rational, mechanism-based treatment for hematologic malignancies?" Blood **96**(5): 1655-69.
6. Rodriguez-Viciana, P., P. H. Warne, et al. (1994). "Phosphatidylinositol-3-OH kinase as a direct target of Ras." Nature **370**(6490): 527-32.
7. Vojtek, A. B., S. M. Hollenberg, et al. (1993). "Mammalian Ras interacts directly with the serine/threonine kinase Raf." Cell **74**(1): 205-14.
8. Huang, Y. and R. L. Wange (2004). "T cell receptor signaling: beyond complex complexes." J Biol Chem **279**(28): 28827-30.
9. Chang, L. and M. Karin (2001). "Mammalian MAP kinase signalling cascades." Nature **410**(6824): 37-40.
10. Franke, T. F., D. R. Kaplan, et al. (1997). "PI3K: downstream AKTion blocks apoptosis." Cell **88**(4): 435-7.
11. Bos, J. L., H. Rehmann, et al. (2007). "GEFs and GAPs: critical elements in the control of small G proteins." Cell **129**(5): 865-77.
12. Bernards, A. (2003). "GAPs galore! A survey of putative Ras superfamily GTPase activating proteins in man and Drosophila." Biochim Biophys Acta **1603**(2): 47-82.
13. Donovan, S., K. M. Shannon, et al. (2002). "GTPase activating proteins: critical regulators of intracellular signaling." Biochim Biophys Acta **1602**(1): 23-45.
14. Scheffzek, K., M. R. Ahmadian, et al. (1997). "The Ras-RasGAP complex: structural basis for GTPase activation and its loss in oncogenic Ras mutants." Science **277**(5324): 333-8.
15. Wittinghofer, A., K. Scheffzek, et al. (1997). "The interaction of Ras with GTPase-activating proteins." FEBS Lett **410**(1): 63-7.
16. Bos, J. L. (1989). "ras oncogenes in human cancer: a review." Cancer Res **49**(17): 4682-9.

17. Vojtek, A. B. and C. J. Der (1998). "Increasing complexity of the Ras signaling pathway." J Biol Chem **273**(32): 19925-8.
18. Takai, Y., T. Sasaki, et al. (2001). "Small GTP-binding proteins." Physiol Rev **81**(1): 153-208.
19. Margolis, B., N. Li, et al. (1990). "The tyrosine phosphorylated carboxyterminus of the EGF receptor is a binding site for GAP and PLC-gamma." EMBO J **9**(13): 4375-80.
20. Fantl, W. J., J. A. Escobedo, et al. (1992). "Distinct phosphotyrosines on a growth factor receptor bind to specific molecules that mediate different signaling pathways." Cell **69**(3): 413-23.
21. Ekman, S., E. R. Thuresson, et al. (1999). "Increased mitogenicity of an alphabeta heterodimeric PDGF receptor complex correlates with lack of RasGAP binding." Oncogene **18**(15): 2481-8.
22. Agazie, Y. M. and M. J. Hayman (2003). "Molecular mechanism for a role of SHP2 in epidermal growth factor receptor signaling." Mol Cell Biol **23**(21): 7875-86.
23. Bollag, G. and F. McCormick (1991). "Differential regulation of rasGAP and neurofibromatosis gene product activities." Nature **351**(6327): 576-9.
24. van der Geer, P., M. Henkemeyer, et al. (1997). "Aberrant Ras regulation and reduced p190 tyrosine phosphorylation in cells lacking p120-Gap." Mol Cell Biol **17**(4): 1840-7.
25. Kulkarni, S. V., G. Gish, et al. (2000). "Role of p120 Ras-GAP in directed cell movement." J Cell Biol **149**(2): 457-70.
26. Hu, K. Q. and J. Settleman (1997). "Tandem SH2 binding sites mediate the RasGAP-RhoGAP interaction: a conformational mechanism for SH3 domain regulation." EMBO J **16**(3): 473-83.
27. Ridley, A. J., H. F. Paterson, et al. (1992). "The small GTP-binding protein rac regulates growth factor-induced membrane ruffling." Cell **70**(3): 401-10.
28. Yang, J. Y. and C. Widmann (2001). "Antiapoptotic signaling generated by caspase-induced cleavage of RasGAP." Mol Cell Biol **21**(16): 5346-58.
29. Yang, J. Y. and C. Widmann (2002). "The RasGAP N-terminal fragment generated by caspase cleavage protects cells in a Ras/PI3K/Akt-dependent manner that does not rely on NFkappa B activation." J Biol Chem **277**(17): 14641-6.
30. Yang, J. Y., D. Michod, et al. (2004). "Partial cleavage of RasGAP by caspases is required for cell survival in mild stress conditions." Mol Cell Biol **24**(23): 10425-36.
31. Yang, J. Y., J. Walicki, et al. (2005). "Impaired Akt activity down-modulation, caspase-3 activation, and apoptosis in cells expressing a caspase-resistant mutant of RasGAP at position 157." Mol Biol Cell **16**(8): 3511-20.
32. Henkemeyer, M., D. J. Rossi, et al. (1995). "Vascular system defects and neuronal apoptosis in mice lacking ras GTPase-activating protein." Nature **377**(6551): 695-701.

33. Eerola, I., L. M. Boon, et al. (2003). "Capillary malformation-arteriovenous malformation, a new clinical and genetic disorder caused by RASA1 mutations." Am J Hum Genet **73**(6): 1240-9.
34. Boon, L. M., J. B. Mulliken, et al. (2005). "RASA1: variable phenotype with capillary and arteriovenous malformations." Curr Opin Genet Dev **15**(3): 265-9.
35. Brouillard, P. and M. Vikkula (2007). "Genetic causes of vascular malformations." Hum Mol Genet **16 Spec No. 2**: R140-9.
36. Revencu, N., L. M. Boon, et al. (2008). "Parkes Weber syndrome, vein of Galen aneurysmal malformation, and other fast-flow vascular anomalies are caused by RASA1 mutations." Hum Mutat **29**(7): 959-65.
37. Germain, R. N. (1994). "MHC-dependent antigen processing and peptide presentation: providing ligands for T lymphocyte activation." Cell **76**(2): 287-99.
38. Garcia, K. C., L. Teyton, et al. (1999). "Structural basis of T cell recognition." Annu Rev Immunol **17**: 369-97.
39. Wange, R. L. (2000). "LAT, the linker for activation of T cells: a bridge between T cell-specific and general signaling pathways." Sci STKE **2000**(63): RE1.
40. Ebinu, J. O., S. L. Stang, et al. (2000). "RasGRP links T-cell receptor signaling to Ras." Blood **95**(10): 3199-203.
41. Priatel, J. J., S. J. Teh, et al. (2002). "RasGRP1 transduces low-grade TCR signals which are critical for T cell development, homeostasis, and differentiation." Immunity **17**(5): 617-27.
42. Roose, J. P., M. Mollenauer, et al. (2005). "A diacylglycerol-protein kinase C-RasGRP1 pathway directs Ras activation upon antigen receptor stimulation of T cells." Mol Cell Biol **25**(11): 4426-41.
43. Kondo, M., I. L. Weissman, et al. (1997). "Identification of clonogenic common lymphoid progenitors in mouse bone marrow." Cell **91**(5): 661-72.
44. von Boehmer, H., I. Aifantis, et al. (1998). "Crucial function of the pre-T-cell receptor (TCR) in TCR beta selection, TCR beta allelic exclusion and alpha beta versus gamma delta lineage commitment." Immunol Rev **165**: 111-9.
45. Godfrey, D. I., J. Kennedy, et al. (1993). "A developmental pathway involving four phenotypically and functionally distinct subsets of CD3-CD4-CD8- triple-negative adult mouse thymocytes defined by CD44 and CD25 expression." J Immunol **150**(10): 4244-52.
46. Janeway, C., M. Shlomchik, et al. (2005) Immunobiology: the immune system in health and disease, 6th edition. Garland Scientific Publishing.
47. Marrack, P. and J. Kappler (1997). "Positive selection of thymocytes bearing alpha beta T cell receptors." Curr Opin Immunol **9**(2): 250-5.
48. von Boehmer, H., P. Kisielow, et al. (1989). "The expression of CD4 and CD8 accessory molecules on mature T cells is not random but correlates with the specificity of the alpha beta receptor for antigen." Immunol Rev **109**: 143-51.

49. Punt, J. A., B. A. Osborne, et al. (1994). "Negative selection of CD4+CD8+ thymocytes by T cell receptor-induced apoptosis requires a costimulatory signal that can be provided by CD28." J Exp Med **179**(2): 709-13.
50. Shortman, K., M. Egerton, et al. (1990). "The generation and fate of thymocytes." Semin Immunol **2**(1): 3-12.
51. Barry, M. and R. C. Bleackley (2002). "Cytotoxic T lymphocytes: all roads lead to death." Nat Rev Immunol **2**(6): 401-9.
52. Szabo, S. J., B. M. Sullivan, et al. (2003). "Molecular mechanisms regulating Th1 immune responses." Annu Rev Immunol **21**: 713-58.
53. Murphy, K. M. and S. L. Reiner (2002). "The lineage decisions of helper T cells." Nat Rev Immunol **2**(12): 933-44.
54. Toda, A. and C. A. Piccirillo (2006). "Development and function of naturally occurring CD4+CD25+ regulatory T cells." J Leukoc Biol **80**(3): 458-70.
55. Awasthi, A. and V. K. Kuchroo (2009). "Th17 cells: from precursors to players in inflammation and infection." Int Immunol.
56. Crompton, T., K. C. Gilmour, et al. (1996). "The MAP kinase pathway controls differentiation from double-negative to double-positive thymocyte." Cell **86**(2): 243-51.
57. Pages, G., S. Guerin, et al. (1999). "Defective thymocyte maturation in p44 MAP kinase (Erk 1) knockout mice." Science **286**(5443): 1374-7.
58. Fischer, A. M., C. D. Katayama, et al. (2005). "The role of erk1 and erk2 in multiple stages of T cell development." Immunity **23**(4): 431-43.
59. Rincon, M., R. A. Flavell, et al. (2001). "Signal transduction by MAP kinases in T lymphocytes." Oncogene **20**(19): 2490-7.
60. Dong, C., R. J. Davis, et al. (2002). "MAP kinases in the immune response." Annu Rev Immunol **20**: 55-72.
61. D'Souza, W. N., C. F. Chang, et al. (2008). "The Erk2 MAPK regulates CD8 T cell proliferation and survival." J Immunol **181**(11): 7617-29.
62. Baldari, C. T., G. Macchia, et al. (1992). "Interleukin-2 promoter activation in T-cells expressing activated Ha-ras." J Biol Chem **267**(7): 4289-91.
63. Rayter, S. I., M. Woodrow, et al. (1992). "p21ras mediates control of IL-2 gene promoter function in T cell activation." EMBO J **11**(12): 4549-56.
64. Fields, P. E., T. F. Gajewski, et al. (1996). "Blocked Ras activation in anergic CD4+ T cells." Science **271**(5253): 1276-8.
65. Li, W., C. D. Whaley, et al. (1996). "Blocked signal transduction to the ERK and JNK protein kinases in anergic CD4+ T cells." Science **271**(5253): 1272-6.
66. Wattenberg, B. W. and D. M. Raben (2007). "Diacylglycerol kinases put the brakes on immune function." Sci STKE **2007**(398): pe43.
67. Brannan, C. I., A. S. Perkins, et al. (1994). "Targeted disruption of the neurofibromatosis type-1 gene leads to developmental abnormalities in heart and various neural crest-derived tissues." Genes Dev **8**(9): 1019-29.
68. Ingram, D. A., L. Zhang, et al. (2002). "Lymphoproliferative defects in mice lacking the expression of neurofibromin: functional and biochemical

consequences of Nf1 deficiency in T-cell development and function." Blood **100**(10): 3656-62.
69. Galli-Taliadoros, L. A., J. D. Sedgwick, et al. (1995). "Gene knock-out technology: a methodological overview for the interested novice." J Immunol Methods **181**(1): 1-15.
70. Gu, H., Y. R. Zou, et al. (1993). "Independent control of immunoglobulin switch recombination at individual switch regions evidenced through Cre-loxP-mediated gene targeting." Cell **73**(6): 1155-64.
71. Gu, H., J. D. Marth, et al. (1994). "Deletion of a DNA polymerase beta gene segment in T cells using cell type-specific gene targeting." Science **265**(5168): 103-6.
72. Downward, J., J. D. Graves, et al. (1990). "Stimulation of p21ras upon T-cell activation." Nature **346**(6286): 719-23.
73. Holland, S. J., N. W. Gale, et al. (1997). "Juxtamembrane tyrosine residues couple the Eph family receptor EphB2/Nuk to specific SH2 domain proteins in neuronal cells." EMBO J **16**(13): 3877-88.
74. Kaplan, D. R., D. K. Morrison, et al. (1990). "PDGF beta-receptor stimulates tyrosine phosphorylation of GAP and association of GAP with a signaling complex." Cell **61**(1): 125-33.
75. Pronk, G. J., R. H. Medema, et al. (1992). "Interaction between the p21ras GTPase activating protein and the insulin receptor." J Biol Chem **267**(33): 24058-63.
76. Conti, E. and E. Izaurralde (2005). "Nonsense-mediated mRNA decay: molecular insights and mechanistic variations across species." Curr Opin Cell Biol **17**(3): 316-25.
77. Rodriguez, C. I., F. Buchholz, et al. (2000). "High-efficiency deleter mice show that FLPe is an alternative to Cre-loxP." Nat Genet **25**(2): 139-40.
78. Clausen, B. E., C. Burkhardt, et al. (1999). "Conditional gene targeting in macrophages and granulocytes using LysMcre mice." Transgenic Res **8**(4): 265-77.
79. Hennet, T., F. K. Hagen, et al. (1995). "T-cell-specific deletion of a polypeptide N-acetylgalactosaminyl-transferase gene by site-directed recombination." Proc Natl Acad Sci U S A **92**(26): 12070-4.
80. Rickert, R. C., J. Roes, et al. (1997). "B lymphocyte-specific, Cre-mediated mutagenesis in mice." Nucleic Acids Res **25**(6): 1317-8.
81. Ruzankina, Y., C. Pinzon-Guzman, et al. (2007). "Deletion of the developmentally essential gene ATR in adult mice leads to age-related phenotypes and stem cell loss." Cell Stem Cell **1**(1): 113-26.
82. Charles, M. A., T. L. Saunders, et al. (2006). "Pituitary-specific Gata2 knockout: effects on gonadotrope and thyrotrope function." Mol Endocrinol **20**(6): 1366-77.
83. Alberola-Ila, J., K. A. Forbush, et al. (1995). "Selective requirement for MAP kinase activation in thymocyte differentiation." Nature **373**(6515): 620-3.

84. Swan, K. A., J. Alberola-Ila, et al. (1995). "Involvement of p21ras distinguishes positive and negative selection in thymocytes." EMBO J **14**(2): 276-85.
85. Cantrell, D. A. (2003). "GTPases and T cell activation." Immunol Rev **192**: 122-30.
86. Kisielow, P., H. Bluthmann, et al. (1988). "Tolerance in T-cell-receptor transgenic mice involves deletion of nonmature CD4+8+ thymocytes." Nature **333**(6175): 742-6.
87. Kaye, J., M. L. Hsu, et al. (1989). "Selective development of CD4+ T cells in transgenic mice expressing a class II MHC-restricted antigen receptor." Nature **341**(6244): 746-9.
88. Takeda, S., H. R. Rodewald, et al. (1996). "MHC class II molecules are not required for survival of newly generated CD4+ T cells, but affect their long-term life span." Immunity **5**(3): 217-28.
89. Tanchot, C., F. A. Lemonnier, et al. (1997). "Differential requirements for survival and proliferation of CD8 naive or memory T cells." Science **276**(5321): 2057-62.
90. Ernst, B., D. S. Lee, et al. (1999). "The peptide ligands mediating positive selection in the thymus control T cell survival and homeostatic proliferation in the periphery." Immunity **11**(2): 173-81.
91. Zhu, Y., M. I. Romero, et al. (2001). "Ablation of NF1 function in neurons induces abnormal development of cerebral cortex and reactive gliosis in the brain." Genes Dev **15**(7): 859-76.
92. Finkelman, F. D., T. Shea-Donohue, et al. (1997). "Cytokine regulation of host defense against parasitic gastrointestinal nematodes: lessons from studies with rodent models." Annu Rev Immunol **15**: 505-33.
93. Portnoy, D. A., V. Auerbuch, et al. (2002). "The cell biology of Listeria monocytogenes infection: the intersection of bacterial pathogenesis and cell-mediated immunity." J Cell Biol **158**(3): 409-14.
94. Oliver, G. and K. Alitalo (2005). "The lymphatic vasculature: recent progress and paradigms." Annu Rev Cell Dev Biol **21**: 457-83.
95. Karpanen, T. and K. Alitalo (2008). "Molecular biology and pathology of lymphangiogenesis." Annu Rev Pathol **3**: 367-97.
96. Srinivasan, R. S., M. E. Dillard, et al. (2007). "Lineage tracing demonstrates the venous origin of the mammalian lymphatic vasculature." Genes Dev **21**(19): 2422-32.
97. Oliver, G. and R. S. Srinivasan (2008). "Lymphatic vasculature development: current concepts." Ann N Y Acad Sci **1131**: 75-81.
98. Wigle, J. T. and G. Oliver (1999). "Prox1 function is required for the development of the murine lymphatic system." Cell **98**(6): 769-78.
99. Wigle, J. T., N. Harvey, et al. (2002). "An essential role for Prox1 in the induction of the lymphatic endothelial cell phenotype." EMBO J **21**(7): 1505-13.
100. Kaipainen, A., J. Korhonen, et al. (1995). "Expression of the fms-like tyrosine kinase 4 gene becomes restricted to lymphatic endothelium during development." Proc Natl Acad Sci U S A **92**(8): 3566-70.

101. Jackson, D. G. (2004). "Biology of the lymphatic marker LYVE-1 and applications in research into lymphatic trafficking and lymphangiogenesis." APMIS **112**(7-8): 526-38.
102. Karkkainen, M. J., P. Haiko, et al. (2004). "Vascular endothelial growth factor C is required for sprouting of the first lymphatic vessels from embryonic veins." Nat Immunol **5**(1): 74-80.
103. Makinen, T., T. Veikkola, et al. (2001). "Isolated lymphatic endothelial cells transduce growth, survival and migratory signals via the VEGF-C/D receptor VEGFR-3." EMBO J **20**(17): 4762-73.
104. Karpanen, T., M. Wirzenius, et al. (2006). "Lymphangiogenic growth factor responsiveness is modulated by postnatal lymphatic vessel maturation." Am J Pathol **169**(2): 708-18.
105. Irrthum, A., M. J. Karkkainen, et al. (2000). "Congenital hereditary lymphedema caused by a mutation that inactivates VEGFR3 tyrosine kinase." Am J Hum Genet **67**(2): 295-301.
106. Karkkainen, M. J., R. E. Ferrell, et al. (2000). "Missense mutations interfere with VEGFR-3 signalling in primary lymphoedema." Nat Genet **25**(2): 153-9.
107. Karkkainen, M. J., A. Saaristo, et al. (2001). "A model for gene therapy of human hereditary lymphedema." Proc Natl Acad Sci U S A **98**(22): 12677-82.
108. Gale, N. W., G. Thurston, et al. (2002). "Angiopoietin-2 is required for postnatal angiogenesis and lymphatic patterning, and only the latter role is rescued by Angiopoietin-1." Dev Cell **3**(3): 411-23.
109. Jeltsch, M., A. Kaipainen, et al. (1997). "Hyperplasia of lymphatic vessels in VEGF-C transgenic mice." Science **276**(5317): 1423-5.
110. Enholm, B., T. Karpanen, et al. (2001). "Adenoviral expression of vascular endothelial growth factor-C induces lymphangiogenesis in the skin." Circ Res **88**(6): 623-9.
111. Cao, R., M. A. Bjorndahl, et al. (2004). "PDGF-BB induces intratumoral lymphangiogenesis and promotes lymphatic metastasis." Cancer Cell **6**(4): 333-45.
112. Morisada, T., Y. Oike, et al. (2005). "Angiopoietin-1 promotes LYVE-1-positive lymphatic vessel formation." Blood **105**(12): 4649-56.
113. Tammela, T., A. Saaristo, et al. (2005). "Angiopoietin-1 promotes lymphatic sprouting and hyperplasia." Blood **105**(12): 4642-8.
114. Veikkola, T., L. Jussila, et al. (2001). "Signalling via vascular endothelial growth factor receptor-3 is sufficient for lymphangiogenesis in transgenic mice." EMBO J **20**(6): 1223-31.
115. Makinen, T., R. H. Adams, et al. (2005). "PDZ interaction site in ephrinB2 is required for the remodeling of lymphatic vasculature." Genes Dev **19**(3): 397-410.
116. Huang, X. Z., J. F. Wu, et al. (2000). "Fatal bilateral chylothorax in mice lacking the integrin alpha9beta1." Mol Cell Biol **20**(14): 5208-15.

117. Ayadi, A., H. Zheng, et al. (2001). "Net-targeted mutant mice develop a vascular phenotype and up-regulate egr-1." EMBO J **20**(18): 5139-52.
118. Fruman, D. A., F. Mauvais-Jarvis, et al. (2000). "Hypoglycaemia, liver necrosis and perinatal death in mice lacking all isoforms of phosphoinositide 3-kinase p85 alpha." Nat Genet **26**(3): 379-82.
119. Gupta, S., A. R. Ramjaun, et al. (2007). "Binding of ras to phosphoinositide 3-kinase p110alpha is required for ras-driven tumorigenesis in mice." Cell **129**(5): 957-68.
120. Merrigan, B. A., D. C. Winter, et al. (1997). "Chylothorax." Br J Surg **84**(1): 15-20.
121. Petrova, T. V., T. Karpanen, et al. (2004). "Defective valves and abnormal mural cell recruitment underlie lymphatic vascular failure in lymphedema distichiasis." Nat Med **10**(9): 974-81.
122. Kwon, S. and E. M. Sevick-Muraca (2007). "Noninvasive quantitative imaging of lymph function in mice." Lymphat Res Biol **5**(4): 219-31.
123. Jones, N. and D. J. Dumont (2000). "Tek/Tie2 signaling: new and old partners." Cancer Metastasis Rev **19**(1-2): 13-7.
124. Wakioka, T., A. Sasaki, et al. (2001). "Spred is a Sprouty-related suppressor of Ras signalling." Nature **412**(6847): 647-51.
125. Taniguchi, K., R. Kohno, et al. (2007). "Spreds are essential for embryonic lymphangiogenesis by regulating vascular endothelial growth factor receptor 3 signaling." Mol Cell Biol **27**(12): 4541-50.
126. Dagenais, S. L., R. L. Hartsough, et al. (2004). "Foxc2 is expressed in developing lymphatic vessels and other tissues associated with lymphedema-distichiasis syndrome." Gene Expr Patterns **4**(6): 611-9.
127. Gideon, P., J. John, et al. (1992). "Mutational and kinetic analyses of the GTPase-activating protein (GAP)-p21 interaction: the C-terminal domain of GAP is not sufficient for full activity." Mol Cell Biol **12**(5): 2050-6.
128. Miao, W., L. Eichelberger, et al. (1996). "p120 Ras GTPase-activating protein interacts with Ras-GTP through specific conserved residues." J Biol Chem **271**(26): 15322-9.
129. Saraste, M. and M. Hyvonen (1995). "Pleckstrin homology domains: a fact file." Curr Opin Struct Biol **5**(3): 403-8.
130. Harvey, N. L., R. S. Srinivasan, et al. (2005). "Lymphatic vascular defects promoted by Prox1 haploinsufficiency cause adult-onset obesity." Nat Genet **37**(10): 1072-81.
131. Kleinman, H. K., M. L. McGarvey, et al. (1982). "Isolation and characterization of type IV procollagen, laminin, and heparan sulfate proteoglycan from the EHS sarcoma." Biochemistry **21**(24): 6188-93.
132. Kleinman, H. K., M. L. McGarvey, et al. (1986). "Basement membrane complexes with biological activity." Biochemistry **25**(2): 312-8.

133. Wirzenius, M., T. Tammela, et al. (2007). "Distinct vascular endothelial growth factor signals for lymphatic vessel enlargement and sprouting." J Exp Med **204**(6): 1431-40.
134. He, Y., K. Kozaki, et al. (2002). "Suppression of tumor lymphangiogenesis and lymph node metastasis by blocking vascular endothelial growth factor receptor 3 signaling." J Natl Cancer Inst **94**(11): 819-25.
135. Karpanen, T., M. Egeblad, et al. (2001). "Vascular endothelial growth factor C promotes tumor lymphangiogenesis and intralymphatic tumor growth." Cancer Res **61**(5): 1786-90.